Vol: 3
Issue: 2
September, 2023

ADVANCED LIDAR

Online ISSN: 2791-8572

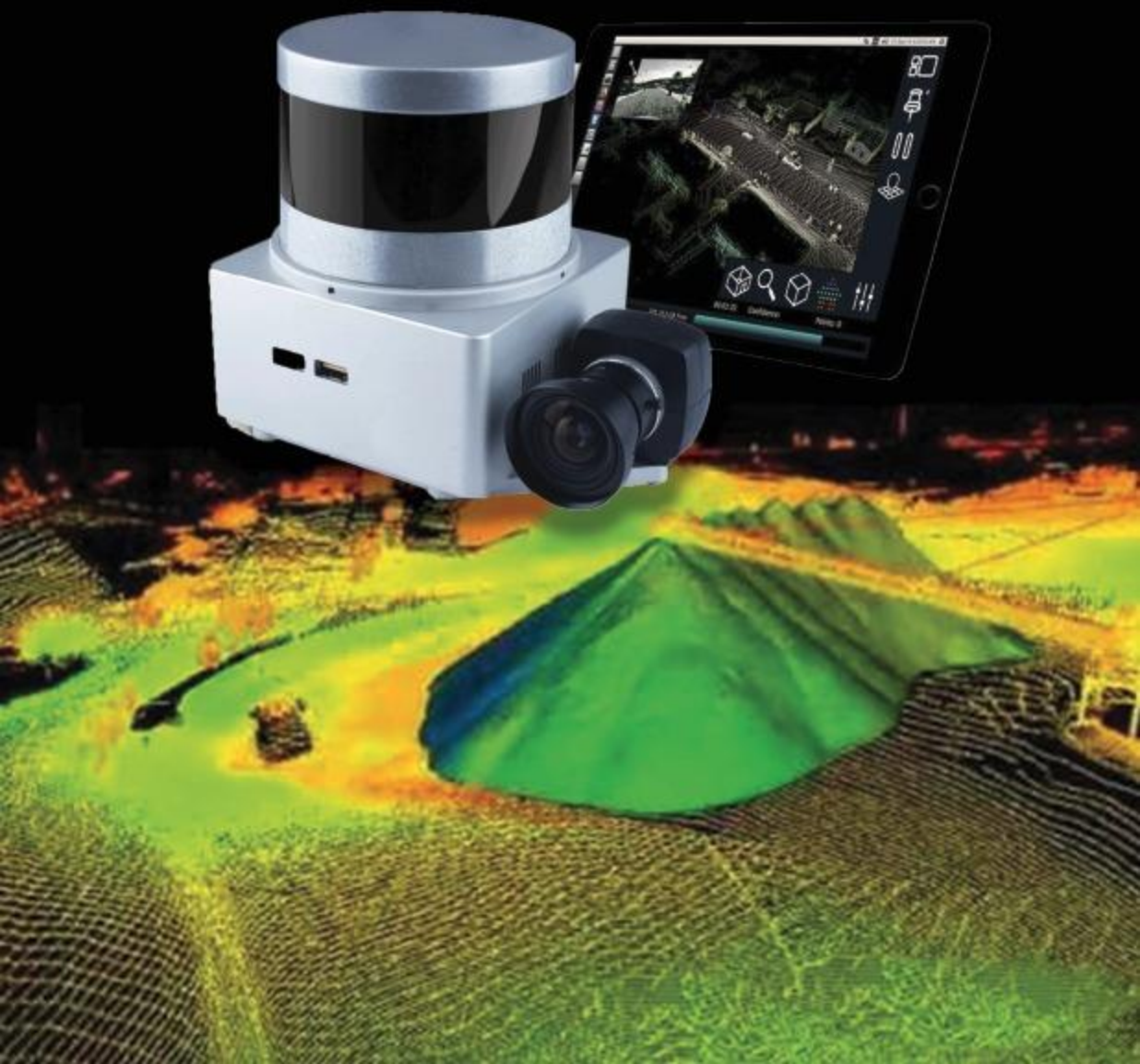

Advanced LiDAR

About Journal

The Advanced LiDAR is a peer-reviewed journal that publishes studies on LiDAR technology development, use, and earth sciences and is scanned in International Indexes and Databases. The journal, LiDAR Systems, and LiDAR Autonom Systems, etc. focuses on the design and applications of LiDAR, including.

Aim & Scope

Turkish Journal of LiDAR,

- To present international developments in the use of terrestrial, wearable, UAV, air, and mobile LiDAR to the information of scientists interested in the fields of Map, Geology, Environment, Mining, Urban Planning, Agriculture, archeology, and architecture.
- To provide an easily accessible and wide-ranging discussion environment that will strengthen and accelerate the sharing of knowledge and experience between scientists, researchers, engineers, and other practitioners who are involved in direct or indirect activities with the following topics.
- To contribute to the initiation and development of inter-institutional cooperation with LiDAR technology, which is of great importance in solving problems related to professional developments that can play a role in technological and economic development in the world and in Turkey.

The scope of Turkish Journal of LiDAR;

- ✓ Basic LiDAR Applications,
- ✓ LiDAR Platforms
- ✓ Terrestrial LiDAR Applications
- ✓ Hand-Held LiDAR Applications
- ✓ Mobile LiDAR Applications
- ✓ Wearable LiDAR Applications
- ✓ Air LiDAR Applications
- ✓ UAV LiDAR Applications
- ✓ LiDAR Autonomous Systems
- ✓ Augmented Reality and virtual reality (VR) applications with LiDAR,
- ✓ Geographical Information Systems integration with LiDAR data,
- ✓ Documentation Studies with LiDAR
- ✓ Industrial measurements with LiDAR,
- ✓ Deformation and Landslide Measurements with LiDAR,
- ✓ Mining Measurements with LiDAR,
- ✓ Urbanism and Transportation Planning Studies with LiDAR,
- ✓ Agricultural Applications with LiDAR,
- ✓ Hydrographic Applications with LiDAR,
- ✓ 3D modeling with LiDAR
- ✓ All multidisciplinary studies conducted with LiDAR,

Publication frequency Biannual

WEB http://publish.mersin.edu.tr/index.php/lidar

Contact alid@mersin.edu.tr / ayasinyigit@mersin.edu.tr

Advanced LiDAR

Advanced LiDAR
Volume *3*
Issue *2* *September, 2023*

Contents

Research Articles;*

Advanced LiDAR

http://publish.mersin.edu.tr/index.php/lidar/index

e-ISSN 2791-8572

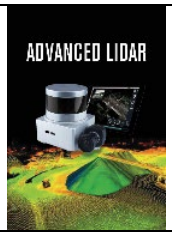

Advantages and Disadvantages of Laser Scanning with ViDoc Rtk Antenna: Ali Cafer Kümbeti

Gonca Büyükmıhçı[1], Ayşegül Akşehirlioğlu[1], Melikşah Koca*[1]

[1]Erciyes University, Faculty of Architecture, Department of Architecture, 38039, Kayseri, Türkiye; (bmgonca@erciyes.edu.tr; aysegul.kilic@erciyes.edu.tr; koca.meliksah@gmail.com)

Keywords

Historical Buildings,
Documentation,
Laser Scanning,
ViDoc RTK.
Ali Cafer Kümbeti

Research Article

Received : 29.12.2022
Revised : 07.07.2023
Accepted : 11.09.2023
Published : 30.09.2023

* **Corresponding Author**
koca.meliksah@gmail.com

Abstract

The first step in accurate and scientific documentation for the preservation of historical buildings is to measure them accurately with a minimum margin of error. Today, with the advancement of technology, laser scanning systems are widely used for this documentation process. With laser scanning, the dimensions, form and details of an architectural structure can be measured and recorded quickly and accurately. Laser scanning systems not only provide measurement data, but also allow the creation of three-dimensional models of these data, providing speed and convenience in the production of project drawings. The data obtained also provides access to wide audiences through the digital archive method in order to protect the structures and transfer them to future generations. IOS mobile laser scanning, a laser scanning technology developed in recent years, has made it possible to perform laser scanning in the documentation of historical buildings using the cameras of IOS devices with Lidar feature. However, since these devices use their own location services, they cause shifts in the images obtained from the scans and make it difficult to place the scans in the coordinate system. Since the use of this method alone does not provide accurate measurement data and increases the margin of error, it requires additional software. In this study, scans performed using the IOS device with the ViDOC RTK (Real Time Kinematics) Antenna were evaluated. Within the scope of the study, the measurement stages of Ali Cafer Kumbet, one of the important components of our cultural heritage, which was scanned using the ViDOC RTK antenna on the IOS device, were examined; the purposes for which the obtained data can be used were determined and their advantages and disadvantages were evaluated.

1. Introduction

Historical buildings are one of the most important representatives of the process in which cultures blend together, and they appear as the most obvious examples reflecting the lifestyles, development levels, beliefs, socio-demographic structures and construction styles of many different civilizations throughout the process. One of the main issues to be focused on is the preservation and transfer to the future of historical buildings which are the determinants of the urban identity and describe the authentic features of the cities that are changing rapidly due to globalization and are in danger of being similar to each other. The most important fact that forms the basis of conservation practices is to ensure the continuity of the building to be preserved without disturbing its original characteristics and in this context, documenting and defining historical buildings correctly constitutes the most important stage of the process.

Traditional methods and technology-supported modern measurement techniques are used for the documentation of historical buildings. Laser scanning systems, which are the subject of the study, are among the modern measurement techniques and allow measurements to be made with a low margin of error.

Cite this;

Büyükmıhçı, G., Akşehirlioğlu, A. & Koca, M (2023). Advantages and Disadvantages of Laser Scanning with ViDoc Rtk Antenna: Ali Cafer Kümbeti. Advanced LiDAR, 3(2), 41-46.

Especially in recent years, digital documentation of cultural heritage has become an area of great importance for researchers. New technologies have facilitated not only professional documentation and scientific management and analysis of data, but also the creation of interactive user-friendly applications for educational and promotional purposes (Barrile et. al., 2019; Shih et. al., 2021). In this context, digital technologies have become an important tool for the promotion and preservation of cultural heritage to a wider audience.

With the development of technology, there have been major evolutionary changes in the techniques used for the collection of 3D data of cultural heritage (Vlachos et al., 2021). Methods that have been used for many years but have recently become popular include terrestrial laser scanning (TLS) and photogrammetry. However, technological innovations such as smartphones, tablets and low-cost sensors have made data collection easier and more affordable (Campi et al., 2021). The versatility, portability and ease use of such devices are the main factors that increase their professional or amateur use as 3D scanning tools. Also, technological advances related to built-in cameras and improved software have improved the quality of images captured with smartphones, thus increasing the quality of 3D models produced from these images (Ortiz et al., 2021). Since 2020, some applications have enabled the widespread use of these techniques by producing products with built-in LiDAR (Light Detection and Ranging) sensors designed specifically for VR and AR (Murtiyoso et al., 2021; Spreafico et al., 2021).

These devices, which contain LiDAR sensors, use their own systems as a location detection method. For this reason, there may be errors or shifts in the images obtained while performing measurements. This can be a serious problem for documentation studies. ViDoc RTK Antenna, which was produced to solve this problem, can be integrated into smart mobile devices with LiDAR sensors. In this way, scans are synchronized directly with PIX4Dcatch. Thus, since the antenna is connected to the NTRIP (Networked Transport of RTCM via Internet Protocol) service, it provides the opportunity to produce 3D models and georeferenced images with real-time RTK accuracy As a result of some studies, it has been seen that data with absolute accuracy less than 5 cm were obtained in the data obtained from the scans made with the ViDOC RTK Antenna. (Atay Engineering, 2023). Within the scope of the article, Ali Cafer Kumbet located in Kayseri Melikgazi District was scanned with the ViDOC RTK Antenna, and the advantages and disadvantages of the system were evaluated over the data obtained during and after the field study.

2. Method

2.1. Ali Cafer Kumbet

Located in a park in Kılıçarslan Neighborhood in the Melikgazi district of Kayseri, the kumbet, which is an important cultural heritage, was built using ashlar stone material on rubble stone filling. The octagonal body with a pyramidal cone was placed on a square-shaped funerary/ burial ground (Şahin, 2021) (Figure 1).

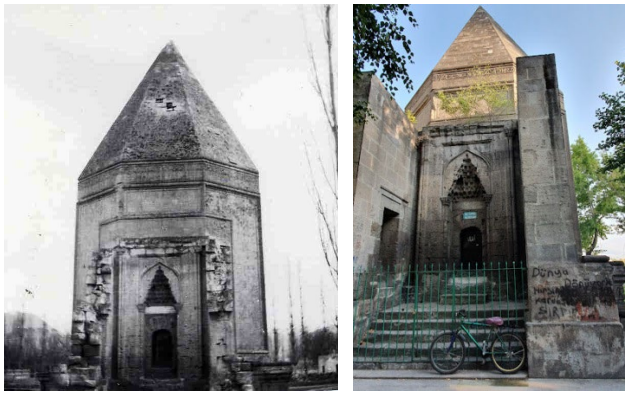

Figure 1. Ali Cafer Kumbet in its old and present state (VGMA, ASÜA, Personal Archive, 2022).

On the north facade are the iwan methal area and the crown gate of the kumbet, and there is a rectangular window on the methal walls (Figure 2). The square portico is accessed by stairs and the octagonal main hall is covered by a round dome. The facades are separated by borders and decorated with rectangular windows having pointed pediments.

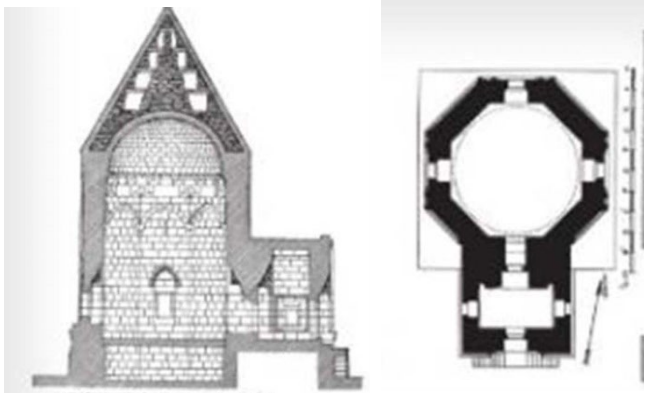

Figure 2. Section and floor plan of Ali Cafer Kumbet (Kayseri Cultural Inventory, 2015).

The building was registered as a monument with the Foundation Old Work Record Form created in the 1960s. At the time of the survey, it is stated that a large part of the portico section forming the entrance was demolished and can be identified by photographs (VGMA) (Figure 3).

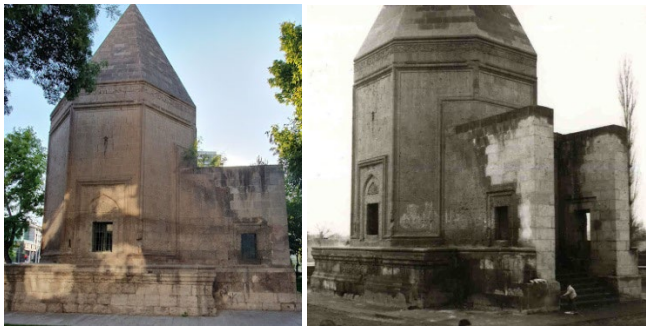

Figure 3. Ali Cafer Kumbet, old and present (VGMA, Personal Archive, 2022).

The exact construction date of the kumbet, which is one of the works that made Kayseri an important Seljuk city, is unknown due to the absence of any inscription on the building. Ali Cafer Kumbet, which is thought to have been built during the Eretnian period, is dated to the

XIVth century (Yanar, 2021; Gabriel, 1931). There is no source on Ali Cafer, to whom the construction and the name are attributed, and there are different opinions on the date of construction. Halil Edhem dates the construction of the kumbet to the Seljuk period, Tamara Talbot Rice to 1247-48, Mahmut Akok to the late XIII. century, Oktay Aslanapa and Ernst Diez to the middle of the XIV. century. (Diez & Aslanapa, 1955; Rice, 1961; Akok, 1970; Edhem, 1982).

2.2. Laser Scanning Studies with ViDoc RTK Antenna

The ViDoc RTK antenna is a real-time satellite data acquisition antenna that can be mounted on mobile smart devices equipped with LiDAR sensors. Synchronized with Pix4Dcatch, the antenna allows the production of RTK-accurate geo-referenced images and 3D models in real time while connected to any NTRIP service (URL A).

Designed by a German company, the viDoc RTK antenna is designed for maximum accuracy and works with Pix4Dcatch software for image acquisition. Handheld and compatible with smart devices, the viDoc RTK antenna is designed to replace expensive ground measurement equipment such as laser scanners to produce 3D final products (URL A). In order to facilitate the perception of a systematic approach to the product acquisition process, the following flowchart was created (Fig.4).

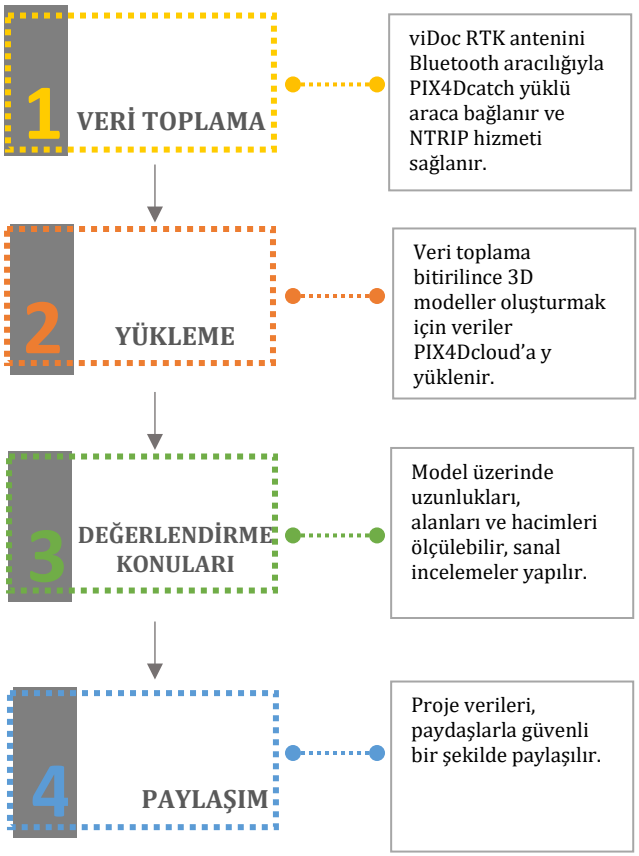

Figure 4. VİDOC RTK Antenna Flow Chart (modified from Atay Engineering).

In the data collection phase, which constitutes the first step according to the flowchart, the device to which the ViDOC RTK Antenna is mounted was connected to the satellite using RTK via PIX4Dcatch before starting the scan. Once it was determined that the connection was stable, the scanning process started (Figure 5).

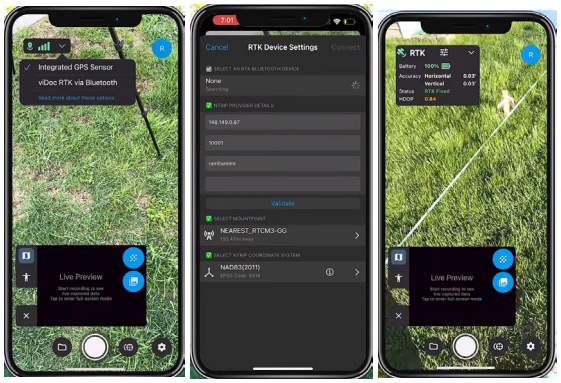

Figure 5. PIX4Dcatch configuration and interface.

Since the height of the building required scanning the building 3 times, the height of the building was divided into four levels and the areas between the determined levels were scanned in different steps. (Figure 6) In order not to cause data drift in the overlays obtained by overlaying the images, extra care was taken not to scan the same area twice or more while scanning.

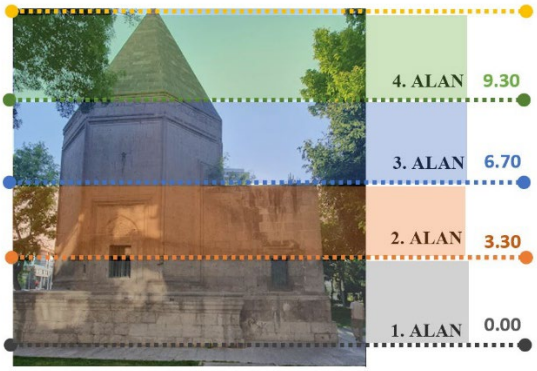

Figure 6. Levels and areas identified for scanning.

For the outdoor scanning, firstly, the device was held at eye level and rotated around the building to scan the 1st area between 0.00 and 3.30 elevations. At the second stage, the device was elevated on a carrying bar and a full-round scan was done. At this stage, the 2nd area between the elevations 3.30 and 6.70 was scanned. Finally, the transport bar was opened all the way and the 3rd area between 6.70 and 9.30 elevations, which are the highest points that can be taken by scanning, was scanned. The fourth area could not be accessed and the areas above the 9.30 level could not be surveyed. After the outdoor measurements were completed, the carrying bar was removed and the indoor measurements were started. During the measurements of the interior, due to the plan scheme of the building and lighting problems, the carrying rod could not be used, and therefore data could only be obtained up to 6.70 level in the interior. During the dome and interior scans, the device was kept as stable as possible and vibration was tried to be avoided, but some minor vibrations occurred in the scan data due to external environmental conditions and the potential for deflection of the carrying bar (Figure 7).

Figure 7. Photographs of the scanning process of the outdoor and indoor spaces of Ali Cafer Kumbet (Personal Archive, 2022).

3. Results

The data obtained as a result of the scan was processed using the PIX4Dcatch application. In addition to the Ali Cafer Kümbeti, which is the focus of the scan, there are also different objects in the surrounding texture (Figure 8). Due to the fact that the environmental data obtained in the scan overloaded the system, this point cloud data was purged by deleting unnecessary points in the PIX4Dcatch application (Figure 9).

Figure 8. Unpurged version of the Ali Cafer Kumbet point cloud data (North facade).

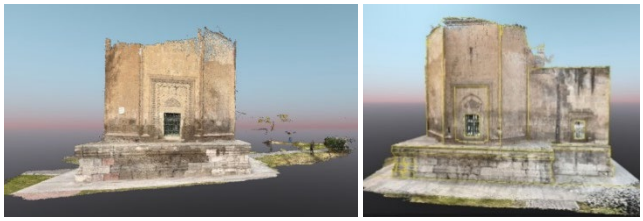

Figure 9. Unpurged and purged Ali Cafer Kumbet point cloud data (East facade).

The obtained data was reduced to a point cloud data consisting of 19666554 points after the cleaning process. The data can be processed in many different applications. However, despite the cleaning process, the data size is still very large, which caused freezes and slowdowns on the computer used when opening the data in various applications. Autodesk Recap Pro and CloudCompare programs were preferred because they are fast and easy to work with and to perform checks and examinations. With the Recap program, not only RGB view of the point cloud data can be obtained, but also views such as "elevation, normal" can be obtained. The Elevation view allows the elevations of the 3D data obtained from the scan to be observed in different colors. This can facilitate data control. The normal view allows a more detailed examination of the surface of the scanned data. These views can be used as support underlays that can facilitate and guide the drawing while performing survey drawings over the point cloud data (Figure 10).

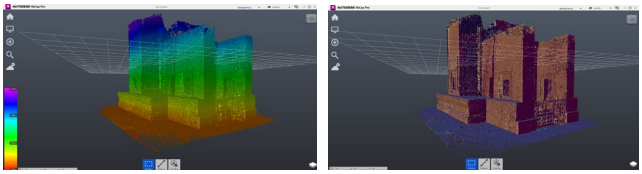

Figure 10. Elevation and normal views obtained from the Recap program

Instead of obtaining a .jpeg underlay over the obtained point cloud data, the point cloud can be imported directly into the Autocad program. In this way, the workload can be reduced while performing the drawings. The point cloud data obtained to create a underlay for the drawings was imported into the Autocad program with the "Insert-Attach" command. After positioning the imported point cloud data, the transformation options were locked so that it would not move during drawing. Then, the "section-two point" command was selected to create section underlays and section points were determined (Figure 11). The same process was repeated for the plan underlays (Figure 12).

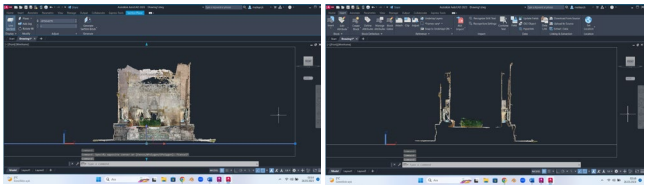

Figure 11. Creation of section underlays by using Autocad program.

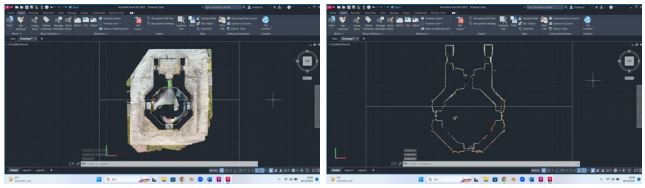

Figure 12. Creation of plan underlays by using Autocad program.

4. Discussion and Conclusion

Within the scope of the study, the Ali Cafer Kumbeti located in the Melikgazi district of Kayseri was scanned with the ViDoc RTK Antenna, an alternative LiDAR scanning method. The ViDOC RTK Antenna, which is integrated into IOS devices with LiDAR capability, aims to produce 3D models with an absolute accuracy of less than 5cm by providing high-precision position detection.

ViDOC RTK Antenna, which can be used instead of laser scanners that provide absolute location service, can be used at low cost as it can be integrated into phones and tablets. The high resolution of the cameras of the phones and tablets that can be integrated with the ViDOC RTK Antenna increases the quality of the product after scanning. At the same time, the PIX4Dcatch application, where data is transferred and processed, offers a simple workflow to the user. In this way, transactions can be solved faster and easier than alternatives. It can also

perform long scanning operations thanks to the lithium batteries inside. Since the method is mobile, it provides opportunities such as portability and fast assembly. Thanks to these opportunities, working time in the field is shortened.

In addition to its many advantages, this scanning system also has some disadvantages. The entire height of the Ali Cafer Kumbet could not be obtained by scanning. Due to the possibilities provided by the carrying stick, a maximum height of 9 meters could be scanned. Since this scanning stick has a thin and long structure, the carrying stick may deflect during measurement. At the same time, the lack of optimization of the data obtained makes it difficult to process the data and transfer it to the 3D model as a mesh surface. High performance computers are needed for this. During the scanning, carrying the device in mobile for a long time tires the person that performing the scan. For this reason, after a certain period of time, there may be shifts in the images obtained in the scan because the device cannot be kept stable.

Table 1. Advantages and disadvantages of scanning with the ViDOC RTK Antenna

Advantages	Disadvantages
It offers scanning at low cost.	In cases where the height of the building is too high, scanning cannot be performed.
The PIX4Dcatch application offers a simple workflow.	The large number of points makes it difficult to process data and work on the mesh surface.
Features such as ease of transportation and fast assembly shorten the working time in the field.	Holding the device steadily in the hand during scanning makes the scanning process difficult.
Lithium batteries enable long scanning operations.	For a good result, the person performing the screening should be experienced and skilled.
Provides absolute position accuracy below 5cm.	

As a result, it was observed that laser scanning with the ViDOC RTK antenna is an efficient system for small-scale structures due to its low cost and mobility, its simple workflow, its ability to perform long scans with lithium batteries, and its absolute position accuracy below 5 cm. However, it has been determined that it can be efficient in medium-scale buildings with the support of equipment such as aerial LiDAR, while it may be inefficient in large-scale buildings.

The advantages and disadvantages of scanning with the ViDOC RTK antenna are given in Table 1 (Table 1). In order to minimize these disadvantages, it is very important to examine the structure or area to be scanned in advance and determine the most effective methods. For example, if structures and groups of structures with high building heights such as the Ali Cafer Kümbet are to be scanned, aerial laser scanning methods should be used in addition to the ViDOC RTK antenna. In order to overcome another disadvantage, which is the high number of points, detailed point cloud cleaning should be performed through the PIX4Dcatch application. At the same time, the use of high-performance computers will facilitate post-scan data processing.

Acknowledgement

We would like to thank Atay Mühendislik for their assistance during the scanning phase.

Author contributions

The authors declare that they have contributed equally to the article.

Conflicts of interest

There is no conflict of interest between the authors.

Statement of Research and Publication Ethics

Research and publication ethics were complied with in the study.

References

Akok, M. (1970). Kayseri'de Dört Mezar Anıtı. *Türk Etnografya Dergisi*, 62, 12-23.

Ali Cafer Kümbeti (2015). Kayseri Kültür Envanteri içinde (1. Baskı, Cilt 1). Kayseri: Kayseri Büyükşehir Belediyesi Kültür Yayınları

Barrile, V., Fotia, A., Candela, G. & Bernardo, E. (2019). Geomatics Techniques for Cultural Heritage Dissemination in Augmented Reality: Bronzi di Riace Case Study. *Heritage*, 2(3), 2243-2254.

Campi, M., di Luggo, A. & Falcone, M. (2021). Photogrammetric Processes and Augmented Reality Applications Using Mobile Devices. *The International Archives of the Photogrammetry, Remote Sensing and Spatial Information Sciences*, XLVI-M (1), 101–106.

Diez, E. & Aslanapa, O. (1955). Türk Sanatı. İstanbul Üniversitesi Edebiyat Fakültesi Yayınları, İstanbul, 80.

Edhem, H. (1982). Kayseri Şehri (Yayına Hazırlayan Kemal Göde). Kültür ve Turizm Bakanlığı Yayınları, Ankara, 131.

Gabriel, A. (1931). Monuments Turcs D'Anatolie I (Kayseri Niğde). De Boccard, Paris, 81

Murtiyoso, A., Grussenmeyer, P., Landes, T. & Macher, H. (2021). First Assessments into the Use of Commercial-Grade Solid State Lidar for Low-Cost Heritage Documentation, ISPRS - International Archives of the Photogrammetry. *Remote Sensing and Spatial Information Sciences*, XLIII(B2), 599–604.

Ortiz-Sanz, J., Gil-Docampo, M., Rego-Sanmartin, T., Arza-García, M., Tucci, G., Parisi, E. I., Bonora, V. & Mugnai,

F. (2021). D3MOBILE Metrology World League: Training Secondary Students on Smartphone-Based Photogrammetry. *ISPRS - International Archives of the Photogrammetry, Remote Sensing and Spatial Information Sciences*, XLIII(B5), 235-241.

Rice, T. T. (1961). The Seljuks in Asia Minor. *Thames and Hudson*, Londra, s.202.

Shih, N.-J, Diao P.-H, Qiu, Y.-T & Chen, T.-Y, (2021). Situated AR Simulations of a Lantern Festival Using a Smartphone and LiDAR-Based 3D Models. *Applied Sciences*, 11(1), 12.

Spreafico, A., Chiabrando, F., Teppati Losè, L., & Giulio Tonolo, F. (2021). The ipad pro built-in lidar sensor: 3d rapid mapping tests and quality assessment. *The International Archives of the Photogrammetry, Remote Sensing and Spatial Information Sciences*, *43*, 63-69.

Şahin, M. (2021). Kayseri Ali Cafer Kümbeti Sorunsalı. Ed: Yılmaz, G., Güner, Y., Güray Gülyüz, B., Uygun Yazıcı, S., Gürkan, E., Seviç, F.) Ortaçağ ve Türk Dönemi Kazılarıve Sanat Tarihi Araştırmaları XXIII içinde (s. 532-546). ISBN: 978-975-374-296-2

Vlachos, A., Polyzou, A. & Economides, A. A. (2022). Photogrammetry with LiDAR iPad Pro. In: Proceedings of EDULEARN 2022, 14th International Conference on Education and New Learning Technologies, 9555-9563. Palma de Mallorca, Spain, 4-6 July. IATED. doi: 10.21125/edulearn.2022.2308

Yanar, Ş. (2008). Türkiye Selçukluları ve Beylikler Devrinde Kayseri'de Kültürel Hayat. Yüksek Lisans Tezi, Sakarya Üniversitesi, Sosyal Bilimler Enstitüsü, 191p (in Turkish)

Advanced LiDAR

http://publish.mersin.edu.tr/index.php/lidar/index

e-ISSN 2791-8572

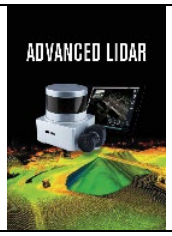

Comparison of CSF Ground Filtering Method by Using Airborne LiDAR Data

Ramazan Alper Kuçak*[1], İsmail Büyüksalih[2]

[1]*Istanbul Technical University, Civil Engineering Faculty, Geomatics Engineering Department, Ayazağa Campus, 34469, Istanbul, Türkiye; (kucak15@itu.edu.tr)*
[2]*Gaziosmanpaşa Municipality, Innovation and Technology Department, 34245, Istanbul, Türkiye; (dr.ibuyuksalih@gmail.com)*

Keywords

Ground Filtering,
LiDAR,
DTM,
CSF,
Point Cloud.

Research Article

Received : 18.05.2023
Revised : 09.08.2023
Accepted : 13.09.2023
Published : 30.09.2023

* **Corresponding Author**
kucak15@itu.edu.tr

Abstract

Airborne LiDAR System (ALS) is a common use of rapid data gathering technologies in a variety of fields, such as cultural heritage, Geography Information Systems (GIS), 3D city modeling, and the production of Digital Terrain Models (DTM). Geomatics experts must use Light Detection and Ranging (LiDAR) to filter out the bare ground from point cloud data. So, the Cloth Simulation Filtering (CSF) ground filtering technique is discussed in this study. The ground and non-ground point clouds of the airborne LiDAR point cloud data were separated for assessment. All point cloud data must be compared for an accurate appraisal of filtering accuracy. However, the data is so massive; this seems implausible. Data manually identified as ground and non-ground were used as a reference to measure classification success adequately. Our findings show that the CSF approach's performance is sufficient but depends on the kind of point cloud, the slope, and the vegetation type.

1. Introduction

In geomatics applications, airborne LiDAR techniques are utilized for rapid data collection on various topographic land surveys. Additionally, many applications have used elevation and geomorphological data from digital elevation models (DEMs) produced by these methods (Erol S. et al., 2020). Large high-resolution regions may be quickly and accurately mapped using LiDAR technology, progressively replacing other methods as the primary way to create Digital Terrain Models (DTMs). On the other hand, DTMs are used to represent the bare soil and validate the actual surface. As a result, point clouds produced by these measurement techniques are increasingly used to create DTMs. DTMs are created by filtering aerial LiDAR point cloud data into the ground and non-ground point clouds. However, point cloud filtering (removing bare soil from point cloud data) remains a significant problem when creating DTMs.

Different ground filtering algorithms have been used in GIS or LiDAR software solutions over the past 20 years (for example, Global Mapper, LASTools, and ALDPAT). However, the advantages of these filtering algorithms differ from terrain to terrain, and each technique employed to cope with various terrains has advantages and disadvantages. In order to choose the best filters, it is advantageous to compare the performance of different filtering algorithms (Chen, C., 2021). However, most algorithms (Klápt, P. et al., 2021; Meng, X., Currit, & Zhao, 2010; Susaki, J., 2012; Rashidi, P., & Rastiveis, H., 2017) are made to filter ALS data. Multiple laser pulse returns are recorded sequentially by the ALS. The ALS records the sequence of multiple laser pulse returns. The values obtained from bare-earth topography that make up the ground points in LiDAR data are typically the lowest surface characteristics in a given locality. Non-ground points are measurements taken from trees, buildings, bridges, and bushes above bare soil. Understanding the physical traits of ground points that set them apart from non-ground points is crucial for correctly identifying them (Xuelian Meng., et al., 2010). As a result, the ground filter algorithm represents the ground using these attributes.

Cite this;

Kuçak, R. A. & Büyüksalih, İ. (2023). Comparison of CSF Ground Filtering Method by Using Airborne LiDAR Data. Advanced LiDAR, 3(2), 47-52.

In post-processing light detection and ranging (LiDAR) data, it is critical to classify the initial point clouds into ground and non-ground points. The cloth simulation filtering (CSF) algorithm is generally used to validate ground points based on physical processes. Cloth simulation is also known as cloth modeling in computer programming. CSF algorithm is an accurate, automatic, easy-to-use LiDAR point cloud algorithm. Particularly, this algorithm's accuracy is similar to the majority of modern ground filtering algorithms. Due to the fact that it has few parameters to process, the users can rapidly implement them with little experience.

Accuracy assessment is essential in ground and non-ground filtering algorithms and its application enhancement. The same test areas are used to evaluate the accuracy of ground filtering algorithms. The accuracy assessment methods of this application have three primary categories, including visual inspection, random sampling of ground-filtered data, and cross tabulation with classified ground truth data (Xuelian Meng., et al., 2010). This study evaluates the CSF algorithm's performance on two LiDAR point cloud data. In addition, it is used to analyze the effects of filtering methods applied to various cloth resolutions. Cloth resolution relates to the grid size of cloth implemented for masking the surface (Zhang et al., 2016).

2. Method

In this study, LiDAR point cloud data were obtained by test flights from 1200 m heights with the Riegl LMS-Q1560 and Optech LiDAR system provided by the general directorate of mapping of Turkey. A manual accuracy assessment approach was preferred for the performance of filtering. The primary purpose of this study is to evaluate the performance of CSF method in different point clouds and different cloth resolutions in the same area.

2.1. Study Area

The case study area for aerial LiDAR data is located in the Bergama test site in Turkey (Figure 1). The land size is 150 m in length and 100 m in width. After obtaining the point cloud data with two different airborne LiDAR systems, the data were processed, and the DTMs were gained with the CSF algorithm's different cloth resolutions for this study area. Furthermore, the accomplishment of the filter algorithms in DTM generation was evaluated and examined.

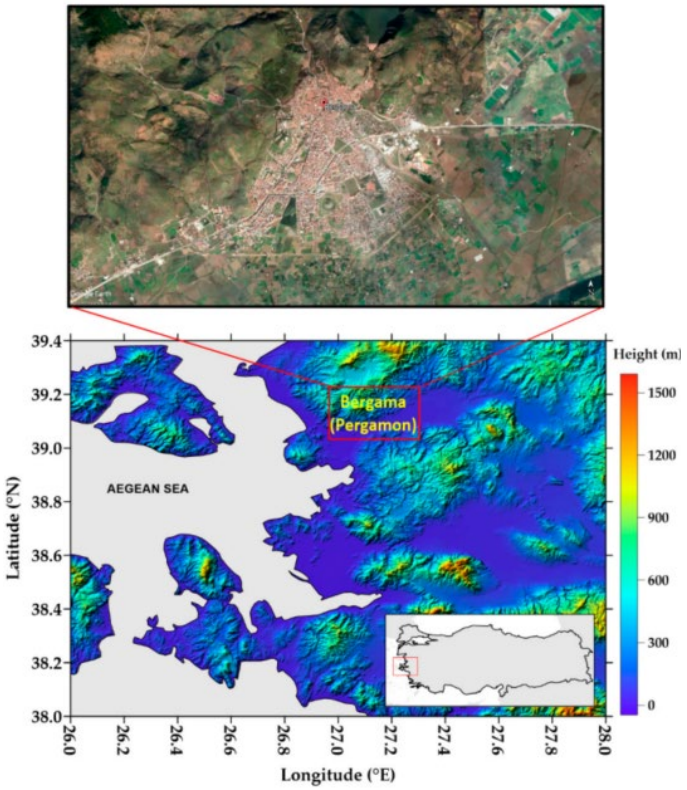

Figure 1. Google Earth image (top) and SRTM DTM (bottom) of Bergama test area (Erol, S. et al., 2021)

2.2. Filtering

In order to create a digital terrain model, filtering is the process of deciding whether data relates to the ground or non-ground surface. Numerous filtering algorithms fall into one of five categories [Buján, S., 2020; Štular, B., & Lozić, E., 2020; Pfeifer, N. and G. Mandlburger, 2018; Süleymanoğlu, B. and Soycan, M., 2019, Kuçak, R. A., 2022):

- Morphological filtering (PMF, SBF, SMRF),
- Surface-based filtering (WLS, CSF),
- Segmentation-based filtering (SegBF),
- Progressive densification (PTIN),
- Other (MCC), and Hybrid (BMHF).

According to Zhang et al. (2016), the CSF algorithm divides point clouds into the ground and non-ground points using a cloth simulation approach. CSF is a cloth simulation-based airborne LiDAR filtering technique. It only attempts to replicate how cloth nodes and accompanying LiDAR points interact. An approximate representation of the ground surface may be created by determining the positions of the cloth nodes. By comparing the original LiDAR points with the produced surface, the ground points may be retrieved from the LiDAR point cloud. Thus, cloth simulation filtering (CSF) could refer to the filtering algorithm (W. Zhang et al., 2016). Figure 2 illustrates the overview of the CSF algorithm.

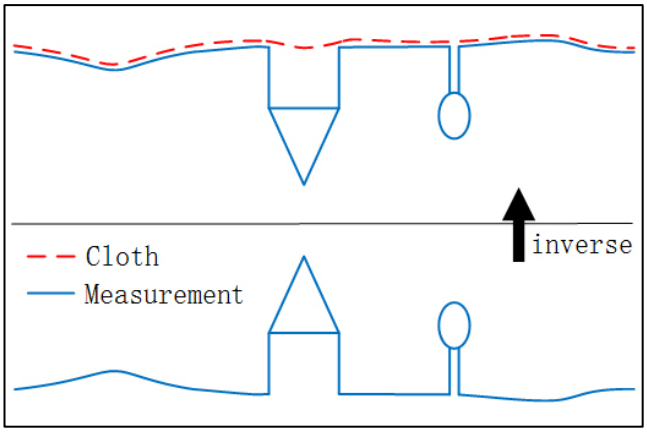

Figure 2. Overview of the CSF algorithm (Zhang et al., 2016).

The point cloud data were filtered using the CSF method in this case study, and DTMs were produced. CSF is built on surface-based filtering methodologies. All points are first acknowledged as ground points; then, all non-ground points are gradually removed. The surface is generally defined using all of the points from the first step using simple kriging. The distance between the ground and non-ground places is an average surface. The separation from the mean surface determines the residual value (Pingel, T. J., 2013; Süleymanoğlu, B. and Soycan, M., 2019, Kuçak, R. A., 2022).

The efficiency of filtering methods was investigated in this study utilizing ground and non-ground data using a manually edited process (Visual inspection). Visual inspection is a widely used manual accuracy evaluation technique when unavailable ground truth data. Error type I, II, and accuracy were three additional indices based on an employed confusion matrix (Table 1), (Susaki, J., 2012). How equations (1), (2), and (3) are represented (Kuçak, R. A., 2022).

$$\text{error type I} = b/(a+b), \quad (1)$$

$$\text{error type II} = c/(c+d), \quad (2)$$

$$\text{accuracy} = (a+d)/(a+b+c+d), \quad (3)$$

Table 1. Structure of Confusion Matrix

		Classified Points	
		Ground Points	Non-ground Points
Reference Points	Ground Points	a	b
	Non-Ground Points	c	d

3. Results

DTM filtering (CSF method) was applied to two aerial LiDAR data sets using Cloud Compare open-source software. The filtering algorithm's correctness was manually examined using reference data. This case study applied the CSF algorithm to Optech and Riegl LiDAR point clouds and filtered ground and non-ground points with both 0.1 and 0.05 cloth resolution.

3.1. CSF Algorithm with 0.1 Cloth Resolution

Firstly, LiDAR point clouds and filtered ground and non-ground points with 0.1 cloth resolution in this case study. Approximately 173.600 points were filtered as ground points for the Optech point cloud. Also, approximately 98.600 points were filtered as non-ground points (Figure 3a). Approximately 134.400 points were filtered as ground points for the Riegl point cloud. Also, approximately 51.000 points were filtered as non-ground points (Figure 3b).

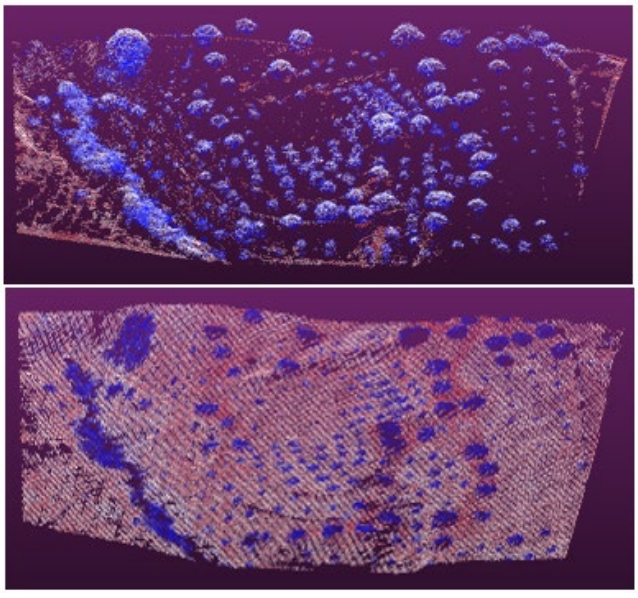

Figure 3a. The ground (bottom) and the non-ground (top) points of Optech Data with CSF 0.1

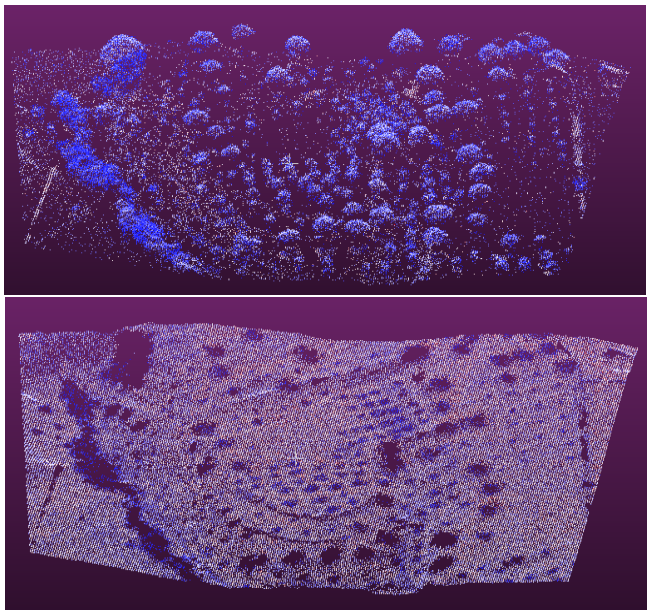

Figure 3b. The ground (bottom) and the non-ground (top) points of Riegl Data with CSF 0.1

3.2. CSF Algorithm 0.05 Cloth Resolution

This case study shows filtered ground and non-ground points with 0.05 cloth resolution. For the Optech Data, approximately 164.300 points were filtered as ground points. Also, approximately 107.800 points were filtered as non-ground points (Figure 4a). Approximately 108.000 points were filtered as ground points for the Riegl point cloud. Also, approximately 77.500 points were filtered as non-ground points (Figure 4b).

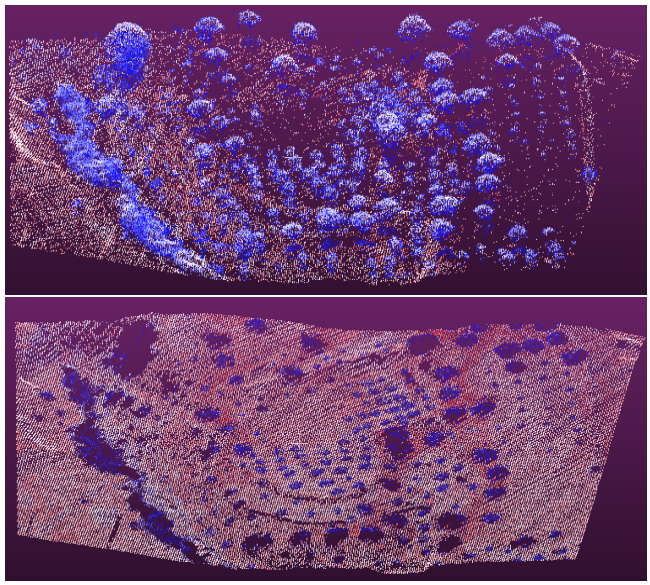

Figure 4a. The ground (**bottom**) and the non-ground (**top**) points of Optech Data with CSF 0.05

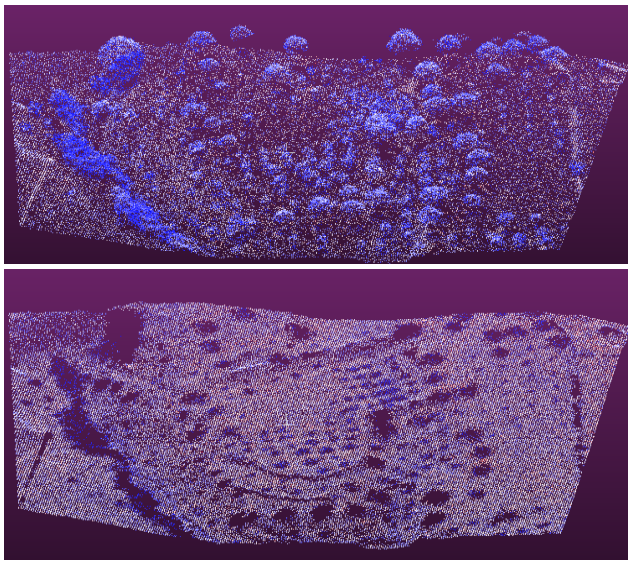

Figure 4b. The ground (**bottom**) and the non-ground (**top**) points of Riegl Data with CSF 0.05

3.3. Evaluation of Filtered Data

Accuracy assessment is essential in ground and non-ground filtering applications and algorithm development. The same test sites are selected to compare and evaluate ground filtering algorithms. Three primary categories of accuracy assessment methods, including visual inspection, random sampling of ground-filtered data, and cross tabulation with classified ground truth data can be used (Xuelian Meng., et al., 2010).

Cloud Compare software was preferred for DTM filtering. The filtering methods were carried out using manually altered reference data, and ground and non-ground data were used as references (Table 1).

The computed type I, type II, and accuracy for the test samples are shown in Table 2. Confusion Matrix has performed with Visual inspection approach. The CSF 0.05 approach has produced the most reliable findings compared to the CSF 0.1 approach. Riegl Lidar CSF 0.05 has the best results with %99 accuracy value for filtering. This case study obtained the most accurate results with CSF 0.05 cloth resolution. This means 0.05 cloth resolution is a more suitable approach for Riegl data. This value needs to be changed to get better results with Optech. This result does not mean the CSF algorithm is inadequate for Optech data. This is a problem for users choosing inappropriate values. As a result, this study also showed that the cloth resolution value in CSF filtering is significant for ground filtering, and the appropriate value should be determined according to the resolution of the point cloud. If care is not taken, ground filtering can cause many errors.

Table 2. The Confusion Matrix of the filtering methods

Sample Dataset	Type I Error (%)	Type II Error (%)	Accuracy
Riegl CSF 0.1	35	17	77
Riegl CSF 0.05	1	1	99
Optech CSF 0.1	48	33	61
Optech CSF 0.05	43	31	63

4. Discussion

Ground and non-ground data were included in the reference data that was performed using the filtering methodologies using the manually filtering approach. The size of the cloth grid used to cover the ground is called the "cloth resolution". The bigger the cloth resolution has set, the coarser DTM will get. On the other hand, different data types cannot use the same cloth resolution. When using the CSF algorithm, the most appropriate value should be chosen by each data because each data's resolution varies. The following factors when selecting workspaces for testing the reliability of ground and non-ground filters should be considered; the difference in slope and elevation, the size and density of objects, the size of the working area, and surface properties. They also affect filtering as they are factors that affect resolution. As a result, this study also demonstrated the importance of the cloth resolution value for ground filtering in CSF filtering and the need to choose the correct value based on the point cloud's resolution. Ground filtering can lead to several mistakes if caution is not applied.

Another factor affecting the comparison of filtering methods is that two different data taken from the same height have a topographic feature in a rural area, that is, without buildings. Natural objects belonging to the earth always provide the best results. Finally, the better result of the Riegl CSF approach can be interpreted differently depending on the parameter changes. However, these results will serve as a reference for future studies.

5. Conclusion

In this study, existing techniques for ground filtering on point clouds are experimentally investigated. These tests highlighted numerous aspects of the methodology by comparing two separate aerial LiDAR datasets with various cloth resolutions. The case study location for aerial LiDAR data is Bergama. The accuracy values for the two datasets and the cloth resolution levels can be adjusted for ground filtering, demonstrating the efficacy of the suggested method for filtering LiDAR data. Shortly, correct filtering can be achieved in both data with correct cloth resolution. These filtering results demonstrated that the suggested strategy might effectively remove non-ground points from LiDAR point clouds.

In future LiDAR filtering applications, novel filtering algorithms for broad fields will be evaluated. The impact of UAV and mobile LiDAR point cloud quality on filtering results will be investigated. The suitable methods for ground filtering will be searched by trying the same algorithms on different data for accurate filtering.

Acknowledgement

The author expresses gratitude to General Directorate of Mapping for providing Airborne LiDAR data.

Author contributions

The authors declare that they have contributed equally to the article.

Conflicts of interest

There is no conflict of interest between the authors.

Statement of Research and Publication Ethics

Research and publication ethics were complied with in the study.

References

Buján, S., Cordero, M., & Miranda, D. (2020). Hybrid overlap filter for LiDAR point clouds using free software. *Remote Sensing*, *12*(7), 1051.

Chen, C., Guo, J., Wu, H., Li, Y. & Shi, B. (2021). Performance Comparison of Filtering Algorithms for High-Density Airborne LiDAR Point Clouds over Complex LandScapes. *Remote Sensing*, *13*(14), 2663.

Erol, S., Özögel, E., Kuçak, R. A. & Erol, B. (2020). Utilizing Airborne LiDAR and UAV Photogrammetry Techniques in Local Geoid Model Determination and Validation. *ISPRS International Journal of Geo-Information*, *9*(9), 528.

Klápště, P., Fogl, M., Barták, V., Gdulová, K., Urban, R. & Moudrý, V. (2021). Sensitivity analysis of parameters and contrasting performance of ground filtering algorithms with UAV photogrammetry-based and LiDAR point clouds. *International Journal of Digital Earth*, *13*(12), 1672-1694.

Meng, X., Currit, N. & Zhao, K. (2010). Ground filtering algorithms for airborne LiDAR data: A review of critical issues. *Remote Sensing*, *2*(3), 833-860.

Pfeifer, N. & G. Mandlburger. (2018). LiDAR data filtering and digital terrain model generation, in Topographic Laser Ranging and Scanning. CRC Press. p. 349-378.

Pingel, T. J., Clarke, K. C. & McBride, W. A. (2013). An improved simple morphological filter for the terrain classification of airborne LIDAR data. *ISPRS Journal of Photogrammetry and Remote Sensing*, *77*, 21-30.

Rashidi, P. & Rastiveis, H. (2017). Ground filtering lidar data based on multi-scale analysis of height difference threshold. *Int. Arch. Photogramm. Remote Sens. Spat. Inf. Sci*, 225-229.

Štular, B. & Lozić, E. (2020). Comparison of Filters for Archaeology-Specific Ground Extraction from Airborne LiDAR Point Clouds. *Remote Sensing*, *12*(18), 3025.

Süleymanoğlu, B., & Soycan, M. (2019). Comparison of filtering algorithms used for DTM production from airborne lidar data: A case study in Bergama, Turkey. *Geodetski Vestnik*, *63*(3).

Susaki, J. (2012). Adaptive slope filtering of airborne LiDAR data in urban areas for digital terrain model (DTM) generation. *Remote Sensing*, *4*(6), 1804-1819.

Zhang, W., Qi, J., Wan, P., Wang, H., Xie, D., Wang, X., & Yan, G. (2016). An easy-to-use airborne LiDAR data filtering method based on cloth simulation. *Remote sensing*, *8*(6), 501.

Meng, X., Currit, N., & Zhao, K. (2010). Ground filtering algorithms for airborne LiDAR data: A review of critical issues. *Remote Sensing*, *2*(3), 833-860.

Advanced LiDAR

http://publish.mersin.edu.tr/index.php/lidar/index

e-ISSN 2791-8572

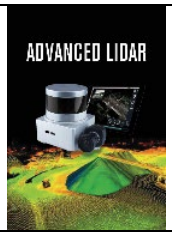

Enhancing Ground Point Extraction in Airborne LiDAR Point Cloud Data Using the CSF Filter Algorithm

Berkan Sarıtaş[1], Gordana Kaplan[*2]

[1]*Eskisehir Technical University, Graduate School of Science, 26555, Eskisehir, Türkiye; (berkansrts@gmail.com)*
[2]*Eskisehir Technical University, Institute of Earth and Space Sciences Institute, 26555, Eskisehir, Türkiye; (kaplangorde@gmail.com)*

Keywords

Remote Sensing,
CSF Filter,
Point Cloud,
SAM,
LIDAR.

Research Article

Received : 03.07.2023
Revised : 22.08.2023
Accepted : 14.09.2023
Published : 30.09.2023

* **Corresponding Author**
kaplangorde@gmail.com

Abstract

Airborne laser scanning (ALS) is a remote sensing method widely recognized for its efficiency in acquiring data quickly and delivering accurate results. To ensure the reliability of ALS data, effective decontamination is crucial. This study aims to enhance the data quality of three distinct LIDAR datasets representing urban, rural, and forest environments by applying the CSF Filter algorithm in the CloudCompare software, an open-source tool widely used in point cloud processing. The impact of various data characteristics and input parameters on the filtering results was assessed through a series of comprehensive tests. The results of our analysis revealed a notable relationship between the selected parameters and the quality of the filtered data. Specifically, when the cover value within the CSF Filter parameters was increased, a corresponding increase in data loss was observed, leading to significantly flawed outcomes. These findings emphasize the importance of carefully selecting and fine-tuning the input parameters to avoid undesirable consequences. The findings underscore the importance of combining automated filtering algorithms with manual cleaning to achieve high-quality and reliable point cloud data for various geospatial analyses and applications.

1. INTRODUCTION

LIDAR is a remote sensing technology, which stands for Light Detection And Ranging (Erişir, 2015). The measurements carried out using LIDAR technology enable the collection of raw data on non-man-made objects and objects that are man-made, that is, all the properties found on the earth's surface (Kostrikov, 2019). 3D digital terrain model (DTM) is a very important resource for determining the details of the earth's surface and preparing projects. The outstanding feature of LIDAR technology as the biggest advantage is revealed when compared with traditional methods of creating numerical models of the earth's surface. These advantages in question are the values of labor, time and accuracy (Karasaka & Keleş, 2020). LIDAR data as point cloud is named. This is due to the fact that the targets have changed and the aircraft being scanned it is due to the irregularity of the scan data as a result of their movements (Lu et al., 2011).

When we look at the areas of use of LIDAR technology, there are two different types of LIDAR: Terrestrial LIDAR and Aerial LIDAR (Çelik et al., 2014).

When LIDAR systems are examined, low cost as well as high point density allows obtaining high and high accuracy reference numerical altitude data, less land studies compared to classical ground measurements and numerical aerial photogrammetry can be shown as advantages of the system (Çelik et al., 2014; Ekercin & Üstün, 2004).

Cite this;

Sarıtaş, B. & Kaplan, G. (2023). Enhancing Ground Point Extraction in Airborne LiDAR Point Cloud Data Using the CSF Filter Algorithm. Advanced LiDAR, 3(2), 53-61.

When the spectral characteristics of the lasers in LIDAR systems are examined, they are located in very wide spectra such as 50-30000 nm from visible and near infrared. The lasers involved in LIDAR systems are limited to the near infrared spectral region. The reason fort his is to reach the data day and night, in the shade or among the clouds (Çelik et al., 2014; Wehr & Lohr, 1999).

Terrestrial Laser Scanning: Terrestrial Laser Scanning (TLS) technology enables the execution of 3D coordinates precisely and automatically (Cömert et al., 2012; Yuriy Reshetyuk, 2009). When examined, it is applied in areas such as registration operations of cultural heritage and engineering projects (Cömert et al., 2012; Lichti & Gordon, 2004).

Aerial Laser Scanning: Modern remote sensing technologies have revolutionized the way we monitor and map large-scale regions, gradually replacing traditional measurement methods. Aerial laser scanning, a prominent laser scanning technology, has emerged as one of the most effective remote sensing methods (Uray 2022). This technique involves transmitting lasers from scanning devices mounted on aircraft or helicopters, which reflect off objects. The distance between the scanning device and the scanned object is then calculated based on the pulse's return time. Aerial LIDAR systems typically comprise three components: GPS, IMU, and a scanner. The scanner records the reflection values, GPS captures location information of the point cloud, and the IMU-derived orientation parameters of the aircraft assist in calibrating the point cloud (Civelekoğlu, 2015).

Remote sensing methods, such as LIDAR, facilitate the creation of numerical elevation models that encompass comprehensive elevation information of the Earth's surface. Models containing three-dimensional information about various structures on the Earth's surface are known as numerical elevation models, while those representing only the bare land surface are referred to as numerical terrain models (Uray, 2022).

LIDAR technology enables the collection of raw data on both natural and man-made objects present on the Earth's surface (Kostrikov, 2019). It allows for rapid and precise acquisition of physical data in a non-contact manner, facilitating the creation of accurate 3D models (Fidan & Fidan, 2021).

The formats of the point cloud data obtained using aerial LIDAR technology may vary, as well as the format often obtained ".las" is an extension structure. When looking at the formats used other than this format, ASCII, .point cloud data can also be obtained in the form of xyz text, fast binary, scan binary and grass sites formats and data processing studies can be performed (Civelekoğlu, 2015; Habib & Rens, 2017).

Point clouds, which are obtained using airborne laser scanning technology, allow us to obtain more information about the terrain than many other sources of data acquisition. Recently, LIDAR point clouds created as a result of obtaining data by airborne (airplane, helicopter) laser scanning are the main data source in order to produce a high-resolution digital surface model (DSM) or digital terrain model (DTM) (Podobnikar & Vrečko, 2012).

This study aims to investigate the performance of different filtering algorithms, specifically focusing on the CSF filter algorithm, in determining ground points for classification in point clouds obtained using LIDAR technology. The research examines various point clouds with distinct properties and compares the accuracy rates of different classification and filtering algorithms. The objective is to determine which algorithm delivers more successful filtering results for specific feature-bearing point clouds.

Previous studies in the literature have employed the CSF filtering algorithm for filtering ground points, such as the study titled "Performance Analysis of the CSF Algorithm for Filtering Ground Points." This research focused on an area characterized by challenging terrain with steep slopes and dense forest cover. Orthophotos obtained simultaneously with the LIDAR data served as reference data for the study. Point cloud data were processed using the CloudCompare software, with specific parameter values selected for filtering operations. The study employed a classification threshold value of 0.5, a repetition time of 1000, and varied grid resolutions of 0.2, 0.3, 0.4, 0.5, 1, and 2. The results demonstrated distortions in the surface model with increasing grid resolution values, resulting in a reduced number of ground-class points. Consequently, manual filtering was deemed necessary to eliminate non-ground points.

By conducting an in-depth analysis of different filtering algorithms, this study contributes to the field of current research topics in LIDAR technology. The findings offer insights into the most effective filtering algorithms for specific types of feature-bearing point clouds, facilitating accurate data analysis and interpretation for various applications (Karasaka & Keleş, 2020).

Looking at another study in the literature, "Assessment of the performance of eight filtering algorithms by using full-waveform LiDAR data of unmanaged eucalypt forest" provides filtering of ground points obtained using the Axelsson filtering algorithm contained in the Terrascan commercial software and seven different filtering algorithms contained in the open-source Aldpat software. The mean value, standard deviation and Roor Mean Squared Error (RMSE) metric values were used to evaluate the weaknesses and strengths of the filtering algorithms. This research focuses on circular plots consisting of brushwood and unmanageable acalyptus forests with different characteristics, where the tree frequency falls by 1600 trees per hectare. In order to evaluate the SAM data generated as a result of the study, a reference SAM surface is created with the help of GNSS receivers. As a result, it is seen that the Axelsson filtering algorithm and the Polynomial Two-Surface Fitting filtering algorithm obtain the highest quality value in terms of RMSE value (Gonçalves & Pereira, 2010).

2. Method

2.1. Point Cloud

In order to be scanned with LIDAR systems, the surface of the objects of the handled area is obtained in 3D. The scanning process is performed systematically,

quickly and automatically, and x, y, z coordinate information for many points can be accessed per second. The set of points obtained by scanning is usually collected as a point cloud during scanning (Gümüş & Erkaya, 2007).

In addition to providing metric and visual or thematic information about an object, a point cloud is the sum of the x, y, z coordinates in the general reference system of objects. If these properties are to be examined, the spatial relationship of the objects between each other and the geometry of the objects, the properties used to Decipher the qualities of the object surface, where metric properties, density or RGB values are found, are called visual or thematic properties (Fröhlich et al., 2000).

2.2. Point Cloud Filtering

The raw LIDAR point cloud contains reflections of all man-made or non-man-made points on the earth's surface (Doğruluk et al., 2018). In order to create a SAM with LIDAR, the points belonging to the ground class must be cleared of objects that do not belong to the ground class, such as trees and buildings. This process in question is called filtering (Soycan et al., 2011b). In order to obtain a high quality surface, it is very important to filter the point cloud in a precise and effective way (Liu, 2008).

When the physical properties of the ground points are taken into consideration, they are grouped in four different ways (Süleymanoğlu & Soycan, 2017; Meng et al., 2010):

- **The lowest height:** Ground points at additional high height in available LIDAR data are the points.
- **The steepness of the floor surface:** When looking at the Declivity between the ground and points that do not belong to the ground, it is steeper than the Declivity between neighboring ground points.
- **The height difference between the decking points:** The high elevation differences of the points between each other indicate the points belonging to objects such as buildings and trees, while the low elevation differences indicate that it is the declivity point.
- **Homogeneity of the floor surface:** The points belonging to the ground are partly smoother and more continuous than the points belonging to other objects.

In the process of creating numerical models consisting of irregular point clouds, processing LIDAR data is an important process. An important stage in the process in question is the filtering of raw LIDAR data. There are many free, open source and many commercial software available for determining the points belonging to the ground class using the filtering algorithms of the LIDAR point cloud. When looking at the literature, it is seen that the strengths and weaknesses of each filtering algorithm stand out for different land surfaces (Karasaka & Keleş, 2020).

Many of the filtering methods use geometric relationships between neighboring points to determine whether the points are on the decking or not. Information such as the pulse width from the exact waveform of the obtained signal, which gives more effective results in areas covered with low vegetation, can improve the desired result (Vosselman & Maas, 2010). The properties of an object that creates a normalized digital surface model (nDSM) and the land surface greatly improve the quality of filtering. There are cases when almost all filtering methods eliminate points that are outside the ground class with difficulty or protect them properly so that DSMs can be created. Examples of these situations are larger buildings, dense vegetation, ramps, bridges, steep slopes, hydrological bodies and different geomorphological edges, i.e. cliffs and riverbanks (Podobnikar & Vrečko, 2012).

A lot of algorithms have been developed for filtering 3D point cloud data. Filtering algorithms are divided into 4 separate groups as Morphological Filtering Algorithms, Gradual Tightening Algorithms, Surface-based Filtering Algorithms and Segmentation-based Filtering Algorithms (Süleymanoğlu, 2016; Briese, 2010).

2.2.1. Morphological filtering algorithms

The filtering algorithms in this group are based on mathematical morphology and are interested in the shapes or shape measurements of objects (Haralick & Shapiro, 1992; Uray, 2016). Various experiments conducted on LIDAR data using morphological filters show that these filters have the ability to distinguish objects outside the ground (Kobler et al., 2007; Uray, 2016). The morphological operators used in the digital image processing are the basic alarm operation, and the operators in question are erosion, expansion, opening and closing. Of these four operators, the wear and expansion operators form the basis of mathematical morphology (Süleymanoğlu, 2016; Haralick & Shapiro, 1992).

2.2.2. Stepwise classification filtering algorithms

It classifies the point cloud data in an iterative manner by starting the filtering process using a small number of point cloud data (Süleymanoğlu, 2016; Briese, 2010). These are algorithms developed based on the principle of smoothness of the floor surface. The points where sudden changes and deviations occur in the point cloud data are considered to be non-ground points. A surface is created using the TIN method from the point cloud data to detect areas where local deviations and sudden changes occur, and thus changes in the surface geometry can be observed accurately (Süleymanoğlu, 2016; Haugerud & Harding, 2001; Meng et al., 2010).

2.2.3. Surface-based filtering algorithms

It uses DSMs created by using the entire dataset for the purpose of filtering point cloud data. In this aspect, it is similar to gradual classification algorithms, but unlike the gradual classification algorithms of surface-based filtering algorithms, instead of adding point data to the ground class step by step, surface-based filtering algorithms initially accept all points as ground points and create temporary DSM using these points. In the next step, the contribution of all points to this surface is reduced, deleted or increased (Süleymanoğlu, 2016; Briese, 2010).

2.2.4. Segmentation and clustering based filtering algorithms

It is based on the approach of classifying point groups by filtering in a collective format instead of classifying points by filtering them one by one (Süleymanoğlu, 2016; Briese, 2010). Points with similarity are included in the same cluster. The classification of the clusters is based on topological relations (Süleymanoğlu & Soycan, 2017; Sithole & Vosselman, 2005).

2.3. Digital Surface Model (DSM)

The numerical surface model can be specified as a model expressed in the 3D coordinate system of XYZ values. DSM is a model formed as a result of showing all man-made and man-made objects that are located on the earth in order to digitally express the earth's descriptive surface. As indicated by the SYMS as a numerical image containing a height value in each pixel, the XYZ values, which are independent of each other and randomly distributed, can also be expressed as a set of triangles that do not intersect each other at known points. With these models, surface areas, volume calculations, slopes and isohips can be used to create (Uray, 2016).

2.4. Digital Terrain Model (DTM)

The term numerical terrain model is defined by the Massacusetts Institute of Technology as a simplified statistical representation of a continuous surface with many points with known XYZ coordinates .(Maliqi et al., 2017; Pedersen, 2022). Models that are used in the same sense as DSM, but are not in vegetation together with all objects that are man-made, are called numerical terrain models. DTM consists of points with high values that better show the true shape of the earth. The material curves obtained using DTM, produced with DSM, show the true shape of the earth in a superior way. DTM is the synonym of DSM for the simple land surface (Maune, 2011; Uray, 2016).

If we look at the areas of use of DTM; There are many areas such as urban planning, forest management, topographic map, transportation, flood hazard and risk maps (Hill et al., 2000; Uray, 2016).

It is possible to produce a numerical terrain model with different interpolation algorithms. The purpose of use and production of the numerical terrain model determines which interpolation algorithm should be used when creating a numerical terrain model. Numerical terrain models produced for geodetic and engineering purposes are commonly represented by a regular grid of points that reproduce the surface heights (GRID), an irregular grid (TIN) and vector lines of the numerical terrain model (Maliqi et al., 2017; Pedersen, 2022). One of them is the slope relief caused by a mathematical operation in the Numerical terrain model raster (Pedersen, 2022; Vosselman & Maas, 2010).

Grid: It is a raster representation of the numerical terrain model on a normal grid. The land surface is represented as a set of elevation values that are related to uniformly distributed X and Y coordinates (Maliqi et al., 2017; Pedersen, 2022)

TIN: It is a numerical terrain model adapted bby multi-GIS software and automatic mapping software (Bjørke, 2010; Pedersen, 2022). TIN models consist of points connected by lines forming triangles, and all triangles form continuous surfaces within them. The surfaces formed are defined by the heights of the three corner points of the triangles (Maliqi et al., 2017; Pedersen, 2022).

Slope relief: It is a visualization method of the height model. These show local elevation changes more clearly than an elevation grid (Pedersen, 2022; Vosselman & Maas, 2010).

2.5. Application

In this study, we investigate the effectiveness of the CSF Filter algorithm, implemented in the CloudCompare software, for filtering LIDAR point cloud data with urban, rural, and forest characteristics. By varying the input parameter values, we aim to determine which parameter values yield more accurate ground point classification. The study involves the creation of Surface Models (SAM) for each parameter value applied in the filtering algorithm, followed by an accuracy analysis of the resulting SAMs.

During the acquisition of LIDAR point clouds, atmospheric conditions like fog or rain can lead to the formation of noise points. Manual cleaning methods using the CloudCompare software are employed to remove these noise points. Subsequently, the CSF Filter algorithm, available in CloudCompare, is utilized for ground point classification. The cover value parameter is assessed using different combinations to determine its impact on the filtering results.

Through this research, we aim to identify the most effective parameter values for accurate ground point classification in LIDAR point cloud data. The findings will contribute to enhancing the data quality and reliability of LIDAR-based applications in urban, rural, and forest environments. Additionally, the study highlights the importance of pre-processing steps, such as manual noise removal, and provides insights into the optimization of the CSF Filter algorithm for improved point cloud filtering.

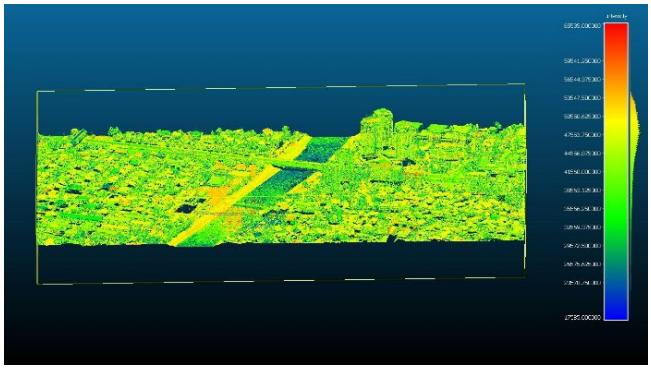

Figure 1. Display of urban area LIDAR data in CloudCompare software

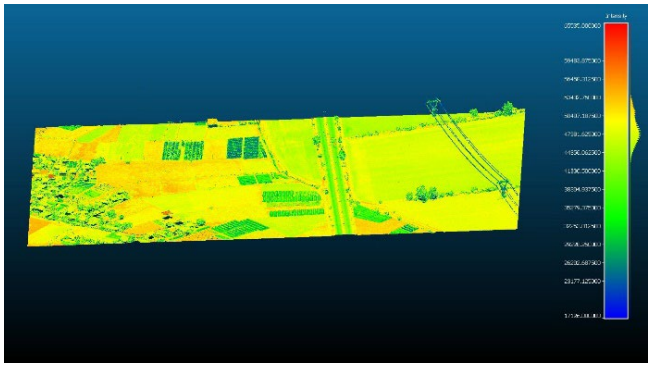

Figure 2. Displaying rural area LIDAR data in CloudCompare software

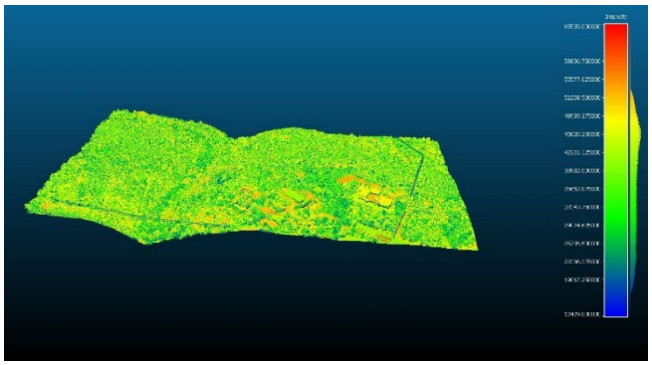

Figure 3. Displaying forest area LIDAR data in CloudCompare software

2.5.1. Filtering of LIDAR data – urban area

The urban area (300 ha) is comprised of an urban area with a total of 312 buildings in the west part of the city of Skopje, the capital of North Macedonia (Figure 1). The study area is divided into two parts, with the Vardar river with a width of approximately 60 m. The left part of the study area contains dense and low residential grid-like buildings with a maximum of 10 m height, while on the right side, there are higher residential and commercial buildings with a maximum height of 70 m. The urban area is generally flat, and the surface elevation of the study area varies from 250–327, while the terrain elevation is from 250–325. Besides buildings, the study area contains many trees, three bridges, and a riverbank of 20 m in width from both sides (Kaplan et al. 2022).

The study area is located in a high-risk seismic zone with a history of destructive earthquakes. Thus, a shallow, magnitude 6.1 earthquake with an intensity rating of IX (Mercalli scale) hit the city in 1963, when the disaster caused significant loss of life and property. More than 1,000 people have been killed, 4,000 injured and more than 200,000 displaced (Kaplan et al., 2022).

Almost %80 of the city was destroyed, and many public buildings, schools, hospitals and historical sites were seriously damaged. More recently, in 2016, a powerful, magnitude ML5.3 earthquake struck the capital (Kaplan et al., 2022; Sinadinovski et al., 2022).

The LIDAR data were obtained from the Cadastre Department of North Macedonia. Data collection was carried out with an aerial platform, Cessna 402B and Riegl VQ-780i sensor system. The data collection was carried out on May 3, 2019 under a clear sky and an air temperature of 11 ° C. The soil sampling distance of LIDAR data is 5 points / m2 (Kaplan et al., 2022).

Figure 5. The study area in city of Skopje, used for the analyses (Adjiski et al., 2023)

Table 1. Number of LIDAR point cloud points in the urban area

Cloth Resolution	Number of LIDAR Points
Original Data	4,537,424
0.1	2,878,720
0.5	2,373,512
1	2,174,743
2	1,896,947
5	1,557,410

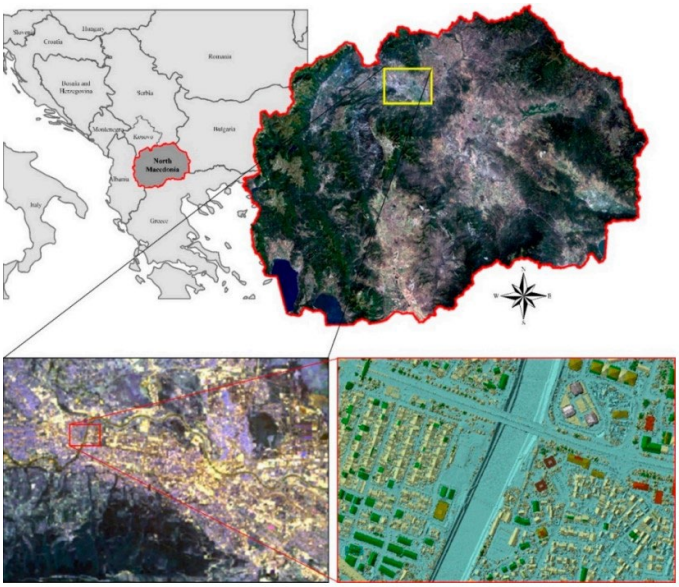

Figure 4. The urban area (Kaplan et al., 2022)

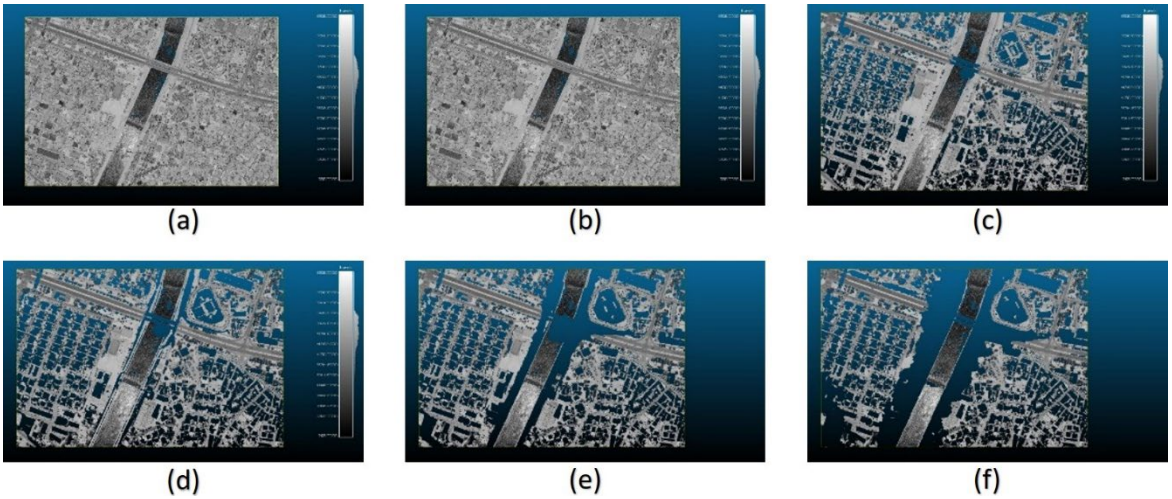

Figure 6. For an urban LIDAR point cloud; (a) The Original Point Cloud, (b) Data Obtained As a Result of Entering the CSF Filter Algorithm Cover Value as 0.1, (c) Data Obtained as a Result of Entering the CSF Filter Algorithm Cover Value as 0.5, (d) Data Obtained As a Result of Entering the CSF Filter Algorithm Cover Value as 1, (e) Data Obtained as a Result of Entering the CSF Filter Algorithm Cover Value as 2, (f) Data Obtained as a Result of Entering the CSF Filter Algorithm Cover Value as 5.

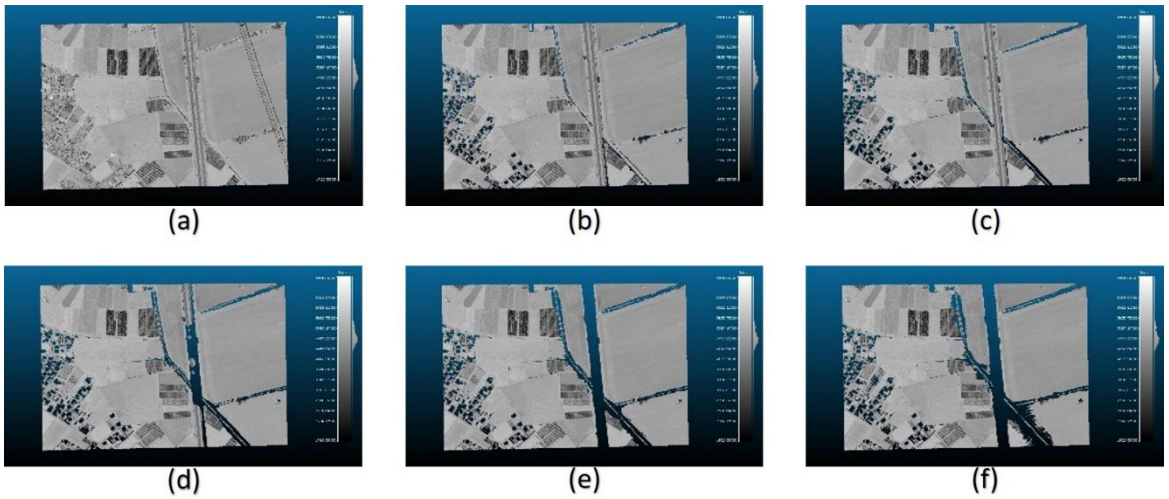

Figure 7. For rural LIDAR point cloud; (a)The Original Point Cloud, (b)The Data Obtained As a Result of Entering the CSF Filter Algorithm Cover Value as 0.1, (c) The Data Obtained as a Result of Entering the CSF Filter Algorithm Cover Value as 0.5, (d) The Data Obtained as a Result of Entering the CSF Filter Algorithm Cover Value as 1, (e) The Data Obtained as a Result of Entering the CSF Filter Algorithm Cover Value as 2, (f)The Data Obtained as a Result of Entering the CSF Filter Algorithm Cover Value as 5.

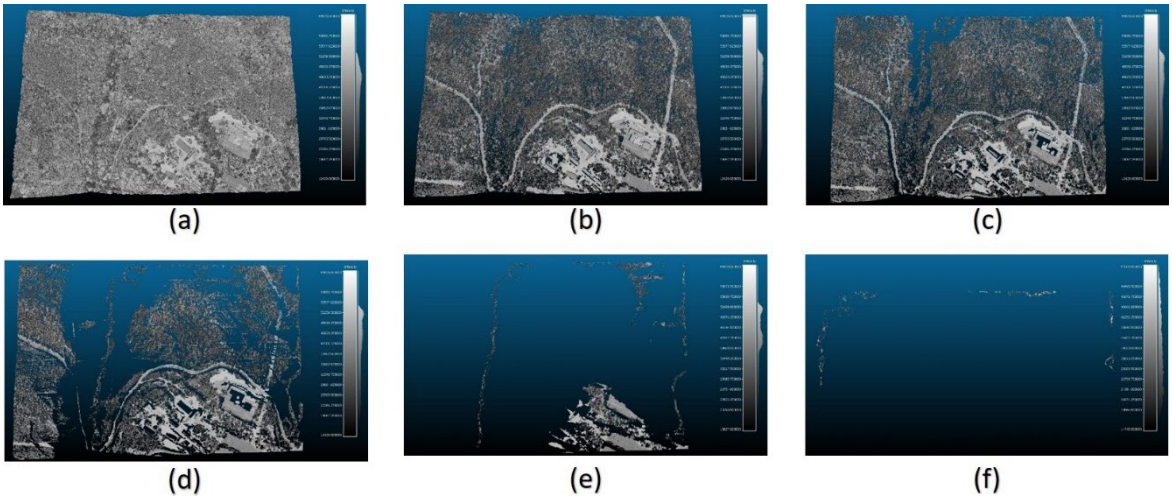

Figure 8. For Forest LIDAR point cloud; (a)The Original Point Cloud, (b)The Data Obtained As a Result of Entering the CSF Filter Algorithm Cover Value as 0.1, (c) The Data Obtained as a Result of Entering the CSF Filter Algorithm Cover Value as 0.5, (d) The Data Obtained as a Result of Entering the CSF Filter Algorithm Cover Value as 1, (e) The Data Obtained as a Result of Entering the CSF Filter Algorithm Cover Value as 2, (f) The Data Obtained as a Result of Entering the CSF Filter Algorithm Cover Value as 5.

2.5.2. Filtering of LIDAR data – rural area

The agricultural study area is flat and consists of corp fields, divided with a road. The main part of the crops are empty, while smaller part of the area consist of green crop lands.

Table 2. Number of LIDAR points cloud points in the rural area

Cloth Resolution	Number of LIDAR Points
Original Data	4,277,552
0.1	3,874,365
0.5	3,823,732
1	3,688,195
2	3,555,055
5	3,453,315

2.5.3. Filtering of LIDAR data – forest area

The forest area is characterized by its abundant growth of dense and towering trees, which create a captivating and enchanting environment. The natural landscape is further enhanced by the presence of rugged mountains.

The terrain within the forest area is undulating, with varying altitudes and steep slopes that add a sense of adventure and challenge to exploring the region.

Table 3. Number of LIDAR points cloud points in the forest ares

Cloth Resolution	Number of LIDAR Points
Original Data	13,952,936
0.1	3,350,703
0.5	2,859,832
1	1,782,871
2	306,483
5	8,293

3. Results

When examining the ground points classified by the CSF Filter algorithm, it becomes evident that there is a loss of data in the ground points as the cover value increases, leading to noticeably incorrect classifications. While it was initially assumed that the decrease in the cover value would accurately determine the actual ground points, it is observed that planar areas such as building roofs are mistakenly classified as ground points.

In assessing the urban, rural, and forest characteristics of the data, it becomes apparent that the most successful results are achieved in rural areas. However, this assessment has been primarily based on visual analysis. In future studies, it is crucial to perform a statistical accuracy assessment to obtain more reliable and objective results. By conducting such an assessment, the outcomes can be quantitatively compared and analyzed to validate the algorithm's performance across different landscapes.

This statistical accuracy assessment would involve rigorous data analysis and comparison of ground truth data with the algorithm's classifications. Furthermore, the assessment should consider factors like the complexity of urban and forest environments, as they pose additional challenges for accurate ground point classification.

By conducting a thorough statistical accuracy assessment, it will be possible to gain a deeper understanding of the algorithm's limitations and strengths across various landscape types. This assessment will provide more robust evidence to evaluate the algorithm's effectiveness and guide future improvements and optimizations.

In conclusion, while the CSF Filter algorithm exhibits data loss and incorrect classifications in ground points with increasing cover values, a more comprehensive and statistically rigorous accuracy assessment is required to assess its performance accurately. By conducting such an assessment and comparing the results across different urban, rural, and forest landscapes, a clearer understanding of the algorithm's performance can be obtained, leading to further improvements and advancements in the future.

4. Discussion

In the process of removing ground points, which is being performed using the CSF Filter algorithm, manual cleaning operation is required in the remaining parts due to the fact that planar areas are considered as ground. In this way, the process of obtaining ground points will reach a more accurate result.

5. Conclusion

In order for the accuracy analysis to be performed with more precise results, reference SAM data are needed. As a result of comparing the obtained data with the reference data, the accuracy rates of the parameters will be determined more accurately.

Acknowledgement

This study is adapted from Berkan Saritas's master's thesis.

Author contributions

Conceptualization and design: Berkan Sarıtaş, Gordana Kaplan
Data collection: Gordana Kaplan
Analysis of data and interpretation of results: Berkan Sarıtaş
Writing the first draft of the manuscript: Berkan Sarıtaş, Gordana Kaplan
Review and editing: Gordana Kaplan

Conflicts of interest

There is no conflict of interest between the authors.

Statement of Research and Publication Ethics

Research and publication ethics were complied with in the study.

References

Adjiski, V., Kaplan, G. & Mijalkovski, S. (2023). Assessment of the solar energy potential of rooftops

using LIDAR datasets and GIS based approach. *International Journal of Engineering and Geosciences*, 8(2), 188-199.

Bjørke, J. T. (2010). Digitale terrengmodeller universitetet for miljø og biovitenskap.

Briese, C. (2010). Extraction of digital terrain models. *Airborne and Terrestrial Laser Scanning*, 135-167. https://repositum.tuwien.at/handle/20.500.12708/26779

Çelik, H., Baş, N. & Coşkun, H. G. (2014). Taşkın modelleme ve risk anaizinde LİDAR verisiyle sayısal yükseklik modeli üretimi. *Gümüşhane Üniversitesi Fen Bilimleri Enstirüsü Dergisi*, 4(1), 117. https://doi.org/10.17714/GUFBED.2014.04.009

Civelekoğlu, B. (2015). Hava LİDAR verilerinin sınıflandırılması ve orman ağaçlarına ait öznitelik değerlendirilmesi İstanbul Belgrad Orman Örneği. Master's Thesis, Yildiz Techinical University, Istanbul (in Turkish).

Cömert, R., Avdan, U., Tün, M. & Ersoy, M. (2012). Mimari belgelemede yersel lazer tarama yönteminin uuygulanması (Seyitgazi Askerlik Şubesi Örneği). *Harita Teknolojileri Elektronik Dergisi*, 4(1), 1-18.

Doğruluk, M., Coşkun Aydin, C. & Yanalak, M. (2018). Kırsal alanlarda SYM üretiminde filtreleme yöntemlerinin performans analizi: Hava LİDAR uygulaması; İstanbul Örneği. *Geomatik Dergisi*, 3(3), 242-253. https://doi.org/10.29128/geomatik.414412

Ekercin, S. & Üstün, B. (2004). Uzaktan algılamada yeni bir teknoloji: LİDAR. *HKM Jeodezi Jeoinformasyon Arazi Yönetimi Dergisi*, 0(91), 34-38. https://search/yayin/detay/59216

Erişir, Z. (2015). Nokta tabanlı sınıflandırma yöntemleri ile LİDAR verilerinin sınıflandırılması. Master's Thesis, Yildiz Techinical University, Istanbul (in Turkish).

Fidan, D. & Fidan, Ş. (2021). Yersel lazer tarama teknolojileriyle oluşturulan 3B modellerin akıllı kent uygulamalarında kullanımı: Mersin Süslü Çeşme Örneği. *Türkiye LİDAR Dergisi*, 3(2), 48-57. https://doi.orrg/10.51946/melid.1021819

Fröhlich, C., Mettenleiiter, M., Härtl, F., Dalton, G. & Hines, D. (2000). Imaging laser radar for 3D modelling of real World environments. *Sensor review*, 20(4), 273-282. https://doi.org/10.1108/02602280010351019

Gonçalves, G. R. & Pereira, I. G. (2010). Assessment of the performance of eight filtering algorithms by using full-waveform LİDAR data of unmanaged eucalypt forest. Silvilaser, 187-196. https:/www.researchgate.net/publication/353307644

Gümüş, K. & Erkaya, H. (2007). Mühendislik uygulamalarında kullanılan yersel lazer tarayıcı sistemler. *TMMMOB Harita ve Kadastro Mühendisleri Odası 11.Türkiye Harita Bilimsel ve Teknik Kurultayı* 2-6 Nisan.

Habib, A. & Rens, J. V. (2017). Quality assurance and quality control of LİDAR systems and derived data. Advanced LİDAR Workshop, University of Northern Iowa, 10, 269-294. https://doi.org/10.1201/9781420051438.CH9

Haralick, R. M. & Shapiro, L. G. (1992). Computer and robot vision. In addison wesley: Reading. Longman Publishing Co. Inc. https://scholar.google.com.tr/citations?hl=tr&user=X8NqGhsAAAAJ&view_op=list_works&sortby=pubdate

Haugerud, R. A. & Harding, D. J. (2001). Some algorithms for virtual deforestation (VDF) of LİDAR topographic survey data. *International Archives of Photogrammetry and Remote Sensing*, 211-217. http://pugetsoundLIDAR.org

Hill, J., Graham, L., Henry, R., Cotter, D. & Young, D. (2000). Wide-area topographic mapping and applications using airbone light detection and ranging (LIDAR) technology. *Photogrammetric Engineering and Remote Sensing*, 66, 908-914.

Kaplan, G., Comert, R., Kaplan, O., Matci, D. K. & Avdan, U. (2022). Using machine learning to extract building inventory information based on LİDAR data. *ISPRS International Journal of Geo-Information*, 11(10). https:doi.org/10.3390/IJGI111005117

Karasaka, L. & Keleş, H. (2000). CSF (Cloth simulation filtering) algoritmasının zemin noktalarını filtrelemedki performans analizi. *Afyon Kocatepe Üniversitesi Fen ve Mühendislik Bilimleri Dergisi*, 267-275. https://doi.org/10.35414/akufemubid.660828

Kobler, A., Preifer, N., Ogrinc, P., Todorovski, L., Oštir, K. & Džeroski, S. (2007). Repetitive interpolation: A robust algorithm for DTM generation from Aerial Laser Scanner Data in forested terrain. *Remote Sensing of Environment*, 108(1), 9-23. https://doi.org/10.1016/J.RSE.2006.10.013

Kostrikov, S. (2019). Urban remote sensing wiith LIDAR fort he Smarth City Concept implementation. Visnyk of V. N. Karazin Kharkiv National University, Series 'Geology, Geography, Ecology', 50. https://doi.org/10.26565/2410-7360-2019-50-08

Lichti, D. D. & Gordon, S. J. (2004). Error Propagation in directly georeferenced terrestrial laser scanner point clouds for cultural heritage recording. FIG Working Week.

Liu, X. (2008). Airbone LİDAR for DEM generation: some critical issues. http://Dx.Doi.Org/10.1177/0309133308089496, 32(1), 31-49. https://doi.org/10.1177/0309133308089496

Lu, Y., Wang, X., Zhou, K. & Yang, J. (2011). MATLAB tools for LIDAR data conversion, visualization and processing. In X. He, J. Xu & V.G. Ferreira (Eds), International Symposium on LIDAR and Radar Mapping 2011: Technologies and Applications. https://doir.org/10.2228/12.912529

Maliqi, E., Penev, P. & Kelmendi, F. (2017). Creating and analysing the digital terrain model of the slivovo area using QGIS Sofware. *Geodesy and Cartography*, 43(3), 111-117. https://doi.org/10.3846/20296991.2017137645

Maune, D. (2011). Digital elevaion model (DTM) whiepaper NRCS high resolution elevation data. USDA Natural Resources Conversation Service National Geospatial Management Center.

Meng, X., Currit, N. & Zhao, K. (2010). Ground filtering algorithms for airbone LIDAR data: A review of critical issues. *Remote Sensing*, 2010, 2(3), 833-860. http://doi.org/10.3390/RS2030833

Pedersen, V. F. (2022). Filtering av LIDAR-punktsky for opprettelse av nøyaktig DTM: en prestasjonsanalyse av to punktskybehandlingssystem, Master's Thesis, miljø- og biovitenskapelige universitet.

Podobnikar, T. & Vrečko, A. (2012). Digital elevation model from the best results of different filtering of a LIDAR point cloud. *Transaction in GIS*, 16(5), 603-617. https://doi.org/10.1111/J.1467-9671.2012.01335.X

Reshetyuk, Y. (2009). Self-calibration and direct georeferencing in terrestrial laser scanning. Doctoral Thesis, Royal Institute of Technology (KTH), Department of Transport and Economics Division of Geodesy.

Sinadinovski, C., Markušić, S., Stanko, D., McCue, K. F. & Pekevski, L. (2022). Seismic analysis of moderate size earthquakes recorded on stations at close epicentral distances. *Applied Sciences*, 12(1), 470. https://doi.org/10.3390/APP12010470

Sithole, G. & Vosselman, G. (2005). Filtering of airbone laser scanner data based on segmented point clouds. *Interational Institute for Geo-Information Science and Earth Obseervation*, 66-71. https://research.utwente.nl/en/publications/filteringof-airborne-laser-scanner-data-based-on-segmented-point

Soycan, M., Tunalıoğlu Öcalan, T., Soycan, A. & Gümüş, K. (2011b). Three dimensional modeling of a forested area using aan airbone light detection and ranging method. *Arabian Journal for Science and Engineering*, 36(4), 581-595. https://doi.org/10.1007/S13369-011-0054-8/METRICS

Süleymanoğlu, B. & Soycan, M. (2017). Hava LİDAR verilerinde kullanılan filtreleme algoritmalarının incelenmesi.

Uray, F. (2016). Hava LİDAR nokta bulutu verileri filtreleme algoritmalarının geliştirilmesi ve performanslarının karşılaştırılması. Master's Thesis, Necmettin Erbakan Universiyt, Konya (in Turkey).

Uray, F. (2022). Derin öğrenme tekniklerini kullanarak hava LİDAR nokta bulutlarının sınıflandırılması. Doctoral Thesis, Necmettin Erbakan University, Konya (in Turkey).

Vosselman, G. & Maas, H. G. (2010). Airbone and terrestrial laser scanning. Whittles Publishing. https://www.whittlespublishing.com/Airborne_and_Terrestrial_Laser_Scanning

Wehr, A. & Lohr, U. (1999). Airbone laser scanning – An introduction and overview. ISPRS Journal of Photogrammetry and Remote Sensing, 54(2-3), 68-82. https://doi.org/10.1016/S0924-2716(99)00011-8

Advanced LiDAR

http://publish.mersin.edu.tr/index.php/lidar/index

e-ISSN 2791-8572

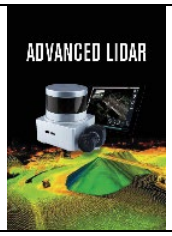

The Use of Terrestrial Laser Scanning Technology in the Documentation of Cultural Heritage: The Case of Bezmialem Valide Sultan Fountain

Berkan Sarıtaş[1], Umut Aydar[*2], Beyza Karademir [2]

[1]Eskisehir Technical University, Graduate School of Science, 26555, Eskisehir, Türkiye; (berkansrts@gmail.com)
[2]Canakkale Onsekiz Mart University, Faculty of Engineering, 17100, Çanakkale, Türkiye; (umutaydar@comu.edu.tr; beyza3992@gmail.com)

Keywords

3-Dimensional Model,
Cloud Compare,
Lidar,
Terrestrial Laser Scanning,
Cultural Heritage.

Research Article

Received : 10.08.2023
Revised : 13.08.2023
Accepted : 16.09.2023
Published : 30.09.2023

* **Corresponding Author**
umutaydar@comu.edu.tr

Abstract

In order to ensure that the structures are repaired again as a result of possible natural disasters and day-to-day wear and tear of historical structures, it is necessary to create 3-dimensional models. One of the methods used in the realization of this model is terrestrial laser scanning. As a result of scanning the historical structures in question in different sessions with the terrestrial laser scanning method, a point cloud is obtained and used in relay studies. The filtering process is performed first for the use of point clouds. The filtering process was carried out by removing the point data found in the environment during the scanning of the structure to be studied and which were considered noise in our study. In our study, CloudCompare software was used in order to turn the point clouds obtained as a result of different sessions and the filtering process completed into a single structure. In order to combine the point clouds, control points established before the scanning process started and natural points located on the structure were used.

1. Introduction

When we look at the geography in which the Republic of Turkey is located, it is determined that it has hosted many civilizations during the historical process. Therefore, the remains of these civilizations are seen quite a lot in the geography. It should never be forgotten that this cultural heritage in question does not belong only to one country, but is a common value of all humanity. It is important that this heritage is protected, repaired and brought to the common heritage of mankind with current technologies (Fidan & Ulvi, 2022).

Cultural heritage are valuable assets that have survived from past generations to us and should be protected and should be passed on from us to future generations, have universal values and have certain criteria. Historical artifacts or historical assets include tangible or intangible cultural and natural heritage (Ulvi et al., 2019; Sarı et al., 2020; Balcı, 2022).

The sustainability of cultural resources can be achieved through conservation and restoration works, and architecture is an important resource. When cultural assets become unable to meet the new demands and needs that are emerging as a result of technological, social and economic changes, new functions can be acquired to ensure their continuity (Aşptekin & Yakar, 2020; Kanun et al., 2021; Kabadayı, 2023). It is very important to ensure the sustainability and protection of cultural heritage (Yakar et al., 2019; Korumaz et al., 2011; Ulvi et al., 2020; Kabadayı, 2023).

In order to be used for repairing damages that may occur as a result of damage to historical structures, terrestrial laser scanning (TLS) technology can be used to create substrates for creating sections of 3-dimensional (3D) models.

Cite this;

Sarıtaş, B., Aydar, U. & Karademir, B. (2023). The Use of Terrestrial Laser Scanning Technology in the Documentation of Cultural Heritage: The Case of Bezmialem Valide Sultan Fountain. Advanced LiDAR, 3(2), 62-69.

Traditional geodetic measurement methods, whole ground measurement or real-time (RTK) GPS measurements are not very suitable for quickly accessing geometric and visual information of the object. These allow only individual point measurement. For this reason, these methods are usually slow. Modern reflector-free total stations and other developing technologies also have point-based scanning functions. However, the excessive scanning time, the low number of points obtained, the inability to obtain sets of points suitable for the actual model of the scanned object have brought the terrestrial laser scanning technology to the forefront (Gümüş & Erkaya, 2007).

There are many basic concepts related to photogrammetry in laser scanning. LIDAR technology forms the basis of laser data production in remote sensing and photogrammetry. It is seen that LIDAR technology stands for light detection and ranging. Light amplification by stimulated emission of radiation describes laser beam technology in its abbreviated form. In terms of the physical structure of the laser beam, it maintains the beam structure over long distances, has a monochromatic and consistent structure. (Gümüş & Erkaya, 2007)

When geometric problems come to the fore in remote sensing and photogrammetry, it is seen that laser scanning technology especially comes to the fore. Laser scanning method, which is essentially LIDAR technology, is an active measurement method. The data obtained by the laser scanning system is a point cloud consisting of 3-dimensional (3D) points (Gümüş & Erkaya, 2007). A large number of X, Y and Z coordinates can be obtained, as well as density information for each point and measurement operations of Red Green Blue (RGB) values are also provided. For all the measured points, x, y and z coordinates are determined in a spherical or ground coordinate system in space (Staiger, 2003; Yakar et al., 2005; Fidan et al., 2022).

The laser scanning technique is called laser scanning by calculating the time elapsed between the laser beam coming out of the laser scanning device hitting the surface of the object to be scanned and then reflected and returned to the device, converting it into distance measurement and decoupling it with the photos taken (Şenol et al., 2021; Kaya et al., 2021; Balcı, 2022). Laser scanner devices are systems that can shoot thousands or millions of laser points per second and detect them back in 3D and convert them into data (Memduhoğlu, 2020; Polat at al., 2020; Balcı, 2022). There are two systems in laser scanning devices: mechanical deflection and laser radar. While the mechanical deflection system records the horizontal and vertical angles of the laser signal, the laser radar system calculates the return time from the surface where the beam transmitted from the scanners hits the scanned object to the device again. The 3D and global coordinate network for laser scanning technology are formed thanks to these two systems (Balcı, 2022). Laser scanning technology is divided into two different classes: aerial laser scanning and terrestrial laser scanning.

Aerial laser scanning (ALS): A laser scanning device is a system consisting of Global Navigation Satellite Systems (GNSS) and Inertial Measurement Unit (IMU) and installed on an aircraft. By scanning objects and surfaces from the air with the help of this system, a point cloud containing coordinate values is obtained (Balcı, 2022).

Today, the horizontal and vertical accuracy of measurements obtained by aerial laser scanning has caught up with photogrammetric methods. The ALS system is mounted on a helicopter, drone or aircraft (Polat & Uysal, 2016).

The scanning device calculates the distance between ground objects and the sensor by recording the Deceleration and return time of the laser beam (Meng et al., 2010). Based on this calculated distance, the current position of the platform is recorded with GNSS, while the position of the object measured is calculated by recording the status of the aircraft with IMU (Liu, 2008).

Terrestrial laser scanning (TLS): It is a technology that is frequently used for the documentation of historical and cultural structures, restoration and survey purposes (Gümüş & Erkaya, 2007). Terrestrial laser scanning is the name of the technology that enables fast and easy data acquisition from objects such as buildings and machines with complex geometry (Staiger, 2003). It provides opportunities for the presentation of 3D photorealistic models, classification of real objects and the creation of visual reality by combining the methods of terrestrial laser scanning technology together with terrestrial image photogrammetry (Forkuo & King, 2004). When compared with traditional measurement techniques, it is seen that 3D point information is a measurement technique that can be obtained with very high speed (Altuntaş & Yıldız, 2008).

Engineering applications of laser scanning technologies in general today (Kanun et al., 2021; Kabadayı, 2023), examination of changes in structures, deformation measurements, measurement of mosques, baths, churches, documentation of cultural heritage such as castles and castles on a city scale (Erdoğan et al., 2021; Kabadayı, 2023), it is observed that it is used in areas such as geography and geological applications such as caves and field research, determining the parameters of forests and woodlands (Alptekin et al., 2019; Kaya et al., 2021b; Kabadayı, 2023).

Laser scanners provide imaging in the form of a point cloud by scanning the object to be measured in the form of arrays of dots under a certain angle in the horizontal and vertical directions. For each laser point, the scanner instrument-centered polar coordinates are measured. These are; the inclined distance to the measured point, the angle that the measuring line makes in the horizontal plane with the x-axis, and the angle of inclination that the measuring line makes with the horizontal plane (Lichti & Gordon, 2004).

If the external surfaces of a building are to be scanned for architectural relay, the tool is installed at any point and the area seen on the building surface is scanned. Then, the scanning is performed by installing the instrument in a suitable place so that it scans the adjacent area of the first scan. Each scan is performed in such a way as to create common scanned areas at a certain rate

with the previous scan. These common scanned areas are necessary for the joining of point sets (Altuntaş & Yıldız, 2008).

Preparation of relay and restoration projects using the terrestrial Laser scanning method; Laser scanning technique was used to create 3D data of the castle ruins in the study entitled Aksehir Castle Ruins Sample. The focus is on obtaining information about the spatial and structural situation through the use of 3D laser scanning technique. When the results of the study are examined, it is seen that the ground laser scanning method is an appropriate and modern technique for collecting special and 3D data in the documentation of historical heritage. With the work carried out, the documentation of the structural and digital data of the castle ruins located in Akşehir was provided (Karadayı, 2023).

In the study entitled three-dimensional (3D) documentation of ancient tombstones by ground laser scanning (TLS) method, it was aimed to digitally document the ancient tombstones that need to be scanned using a scanning device without being exposed to any contact. In the study where ancient tombstones were scanned from different locations, 3D models were produced and visual presentations were created, and thus the documentation of ancient tombstones was completed (Us, 2022).

The aim of my study is to create 3D models as base data for use in repair operations in case of destruction and damage caused by possible natural disasters and day-to-day wear of historical structures.

In order to create 3D models of the Besiktas Valideshcheshme Bezmialem Valide Sultan Fountain, in order to restore the damage that may occur due to damage to historical structures, the measurement process is carried out using the ground laser scanning technique, and the purpose of cleaning the noise points of the scan data obtained is to perform the registration process.

2. Point Cloud

Laser scanning devices, which can be defined as a motorized total station, obtain the surface data of the objects to be scanned in 3D coordinates. The scanning process is performed systematically and automatically and allows reaching the x, y and z coordinates of thousands of points per second. The set of high-accuracy dots obtained from TLS is usually collected as a point cloud during the scan (Mills & Barber, 2003; Gümüş & Erkaya, 2007).

The sum of the x, y and z coordinates of any object or location in the general reference system of spatial distribution is called a point cloud. A point cloud contains various information called ”Metric“ and ”Visual or Thematic": (Mettenleiter, 2000; Gümüş & Erkaya, 2007)

Metric: It Deciphers the object geometry along with showing the spatial relationships between the objects in the environment.

Visual or thematic: There is added information such as density or RGB value. It can be used to calculate the reliability of distance data for each point and to explain the properties of the object surface.

3. The Working Principle of TLS

Terrestrial Laser Scanning devices work with three different principles: those that process with the arrival and departure time of a laser beam, those that process with the phase comparison method, and those that process with the triangulation method. Terrestrial laser scanning devices that process by triangulation method are divided into two different classes as single camera solution and two camera solution.

3.1. Those Who Make Transactions with the Arrival and Departure Time of a Laser Beam

As in total stations, a laser beam is sent to the object to be scanned, and Decalculation of the distance between the instrument sending the laser beam and the surface of the object to be scanned is provided. The measurement of this distance in question is calculated by measuring the departure and arrival time of the laser. Scanning devices use small rotation instruments for the angular deviation of the laser beam and use simple algorithms for calculating lengths. The typical standard deviations of distance measurements are a few millimeters. Due to the relatively short distances, this accuracy is almost the same for the entire object area. The 3D accuracy is also affected by the angular punctuation accuracy of the beam (Boehler, 2002; Gümüş & Erkaya, 2007).

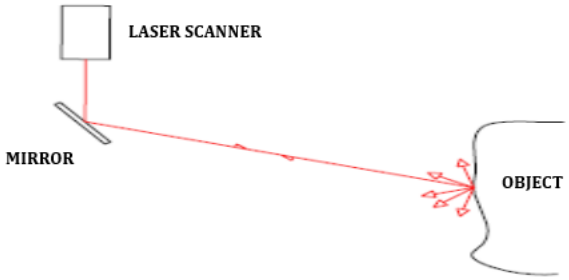

Figure 1. The principle of flight time. (Gümüş ve Erkaya 2007)

3.2. Those Who Make Transactions with the Phase Comparison Method

The transmitted laser is tuned with a compatible wave, and the distance is calculated from the phase deciency between the transmitted and received waves. The results obtained from mixed signal analysis may be more accurate. Since a well-defined return signal is needed, the use of the gas comparison method is more effective at short lengths (Boehler, 2002; Gümüş & Erkaya, 2007).

3.3. Those Who Trade with The Triangulation Method

This method is divided into two different classes: single camera solution and two camera solution.

3.3.1. The Single Camera Solution

Scanners are scanners consisting of a simple beam emitting device.Scanning devices send a laser beam from one end of the mechanical instrument at increasingly

varying angles to the object and with a Charged Coupling Devices (CCD) camera that detects laser points. The 3D positions of the reflective surface elements are obtained from the result triangle. It has priorities in research where range finders are used. From this point of view, the accuracy of the range between the instrument and the object is Decently known along with the distance field. Due to application-related reasons, the base length cannot be increased optionally. These scanners play an important role for short distances and small objects in situations that are more accurate than distance scanners (Boehler, 2002; Gümüş & Erkaya, 2007).

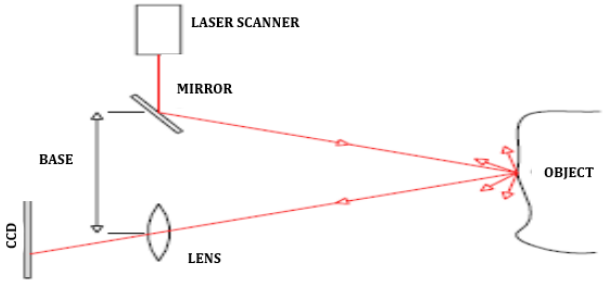

Figure 2. The triangulation principle: A single camera solution. (Gümüş ve Erkaya 2007)

3.3.2. Two Camera Solution

The point or region being examined is produced with a separate light projector that has no measuring function. A broad change of solutions can be seen. The projection consists of a light line of moving ribbon sections. The geometric solution and accuracy results are the same as the single camera principle. Not all instruments that use two cameras provide high ratios and do not produce real-time 3D coordinates. However, if the real-time process of high point rates is provided, these instruments can be considered as an alternative to other specified scanning instruments. (Boehler, 2002; Gümüş & Erkaya, 2007).

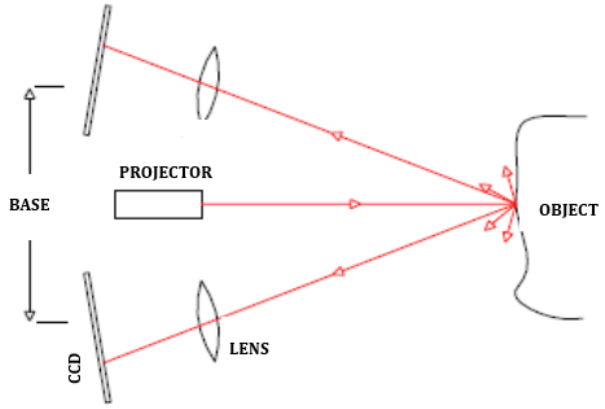

Figure 3. The triangulation principle: Two camera solution. (Gümüş ve Erkaya 2007)

4. TLS DATA STRUCTURE

In the station point instrument-centered coordinate system where TLS are installed, it scans the surface of the object to be scanned in such a way as to obtain the x, y and z cartesian coordinates of thousands of points per second. The data obtained also includes 3D coordinates as well as RGB of the rotating signal depending on the structure of the scanned surface and the measuring distance. Thanks to the recorded RGB density value, it has also become easier to model the scanned object and environment (Altuntaş & Yıldız, 2008).

Laser scanners scan the object to be measured in the form of arrays of dots under a certain angle in the horizontal and vertical direction, allowing it to be displayed as a point cloud. For each laser point, the scanner instrument-centered polar coordinates are measured. These are; the inclined distance to the measured point, the angle that the measuring line makes in the horizontal plane with the x-axis, and the angle of inclination that the measuring line makes with the horizontal plane. Terrestrial laser scanners make measurements based on a completely local coordinate system by accepting the point where they are positioned as the starting point (Lichti & Gordon, 2004).

5. Accuracy of TLS

There are a large number of random errors in the data obtained with laser scanning devices. These errors may be caused by atmospheric conditions, such as measurement system errors caused by beam reflection and beam thickness. By converting the obtained measurements into a geodetic coordinate system, the error amounts caused by the transformation are added to the beam-induced errors. Due to the thickness of the rays sent from the laser scanning device, two different measurement points will be obtained for a laser beam sent from the device, as part of the beam hitting the edge of the scanned object will return to the device, while the remaining part will be reflected from a different surface. By reducing the beam thickness, this error can be reduced to a minimum amount. Atmospheric conditions reduce its effect over short distances. Dust and water vapors will affect the accuracy of the measurements obtained due to the laser beam thickness, and the amount of this error is the same as the amount of error caused by the beam thickness during object edge measurements. This error can also be reduced to a minimum by reducing the size of the laser dot in the same way (Licthi & Gordon, 2004; Altuntaş & Yıldız, 2008).

6. WORKING AREA

Bezmialem Valide Sultan Fountain was built by Bezmialem Valide Sultan on Besiktas Sports Street on the Rumeli side of the Bosphorus in Istanbul in 1839. It is a square fountain with four facades. The fountain was built with the empirical style (URL-1).

The fountain consists of a horizontal wall under the eaves, vertical columns on both sides, an inscription in the middle and a mirror stone under the inscription. Under the eaves with a flat outward flood, there is a fire that rotates along the fountain facades. In the middle of this fire, there is an oval rosette with Sultan Abdulmecit's tugra and a leafy branch motif. There is a horizontal ornament consisting of leaves and tree of life motifs symmetrically on both sides in this fire. There are columns on both sides, one side of which is grooved. In

the middle there is an inscription of five lines in a rectangular frame. There is a column at the corners of the facades, vertical fugues have been placed to give the impression that it consists of 12 rows of stones to reduce the visual effect of this column (URL-1).

In the middle of the facade, there is a mirror stone in a rectangular frame with decorations that show exactly the characteristics of the empirical style. Again, high relief leaf decorations are seen emerging from a large girland motif wrapped with a ribbon at the top. Under the Girland motif, there are two torches in the form of high reliefs. These torches are placed crosswise. The tap comes out of a decorated cabaret. It is enclosed in a rectangular frame arranged with floral reliefs on both sides and with floral reliefs on the quadrilateral. Its convex boat is sturdy. On the horizontal rectangular consoles located under the columns, reliefs with rosettes in the middle and herbal decorations on both sides are placed (URL-1).

There is a number of inscriptions in the fountain. The inscriptions on the two facades of the fountain are written on a mirror stone and are enclosed in a frame with gradual erasures. The verses of the inscriptions are Şükri and Ziver (URL-2).

7. Method

TLS was used to create a 3D point cloud of Bezmialem Valide Sultan Fountain. First of all, control points have been established on the structure in order to be able to use it during the merging of scanning data. The scans were performed in the local coordinate system and eight different scanning operations were performed. During the scanning operations, it was taken into account that there were overlays between consecutive scans, that is, there were common control points Decoupled in the scanning data.

Table 1. The number of points obtained as a result of the sessions

Session Number	Number of Points
1	15.205.100
2	4.244.223
3	3.357.137
4	5.093.182
5	2.723.777
6	11.044.989
7	8.572.569
8	12.438.232

The data obtained as a result of the scanning process are in the ".imp" format. In order to process the data, it is necessary to convert from ".imp" format to ".ptx" format. For the format change, the data with the extension ".imp" transferred to the viewer version of the Leica Cyclone software is recorded in the ".ptx" format without any processing in the software. the data in the ".ptx" format is transferred to the CloudCompare software, which is a free software, and the necessary operations are carried out.

During the scanning of the structure, objects in the environment are included in the scanning data. Points other than the structure should be cleaned both because of the high size of the data and because it causes difficulties to the operator during the processing of the data. The filtering operations were carried out manually with the help of CloudCompare, a free software. After only the data belonging to the structure remains in each session, the registration process is performed using CloudCompare software again so that a 3D model of the object can be created. During sequential scanning, the control points common to both scans are matched.

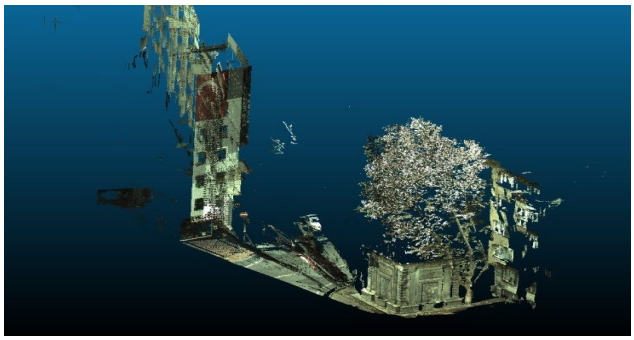

Figure 4. The point cloud obtained as a result of the first session

Figure 5. The point cloud obtained as a result of the second session

Figure 6. The point cloud obtained as a result of the third session

Figure 7. The point cloud obtained as a result of the fourth session

Figure 8. The point cloud obtained as a result of the fifth session

Figure 9. The point cloud obtained as a result of the sixth session

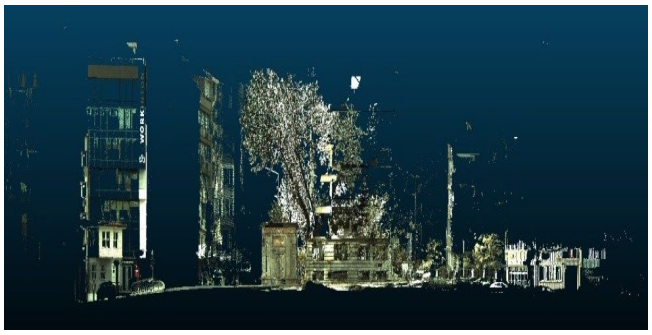

Figure 10. The point cloud obtained as a result of the seventh session

Figure 11. The point cloud obtained as a result of the eighth session

7.1. Filtering the Noise from Point Cloud

Since the work is being performed for a specific object, it is necessary to clear the noise points around that object. The reason for cleaning the noise points is that high-capacity computer technology is needed due to the very large data size and allows the operator, who processes the data obtained as a result of laser scanning, to better distinguish the data and perform more accurate operations. By deleting the noise points, correct interventions can be made to the detail points. Since there will be a significant reduction in the size of the cleared data, time savings will be achieved by reducing the time spent on transactions.

The point cloud data for each scan goes through the filtering process separately. After the data is transferred to the CloudCompare environment, the segment button is selected and the points belonging to the structure that want to be filtering of noise points are surrounded in such a way as to form a closed polyline. By deleting the points remaining outside the selected parts, it is ensured that the noise points remaining around the structure are filtered. In the same way, it is possible to delete the selected parts by selecting noise points. The point cloud is examined from different angles and the filtering process continues until the noise points are detected and only the points belonging to the structure are left. This process is repeated for scanning data for all fronts.

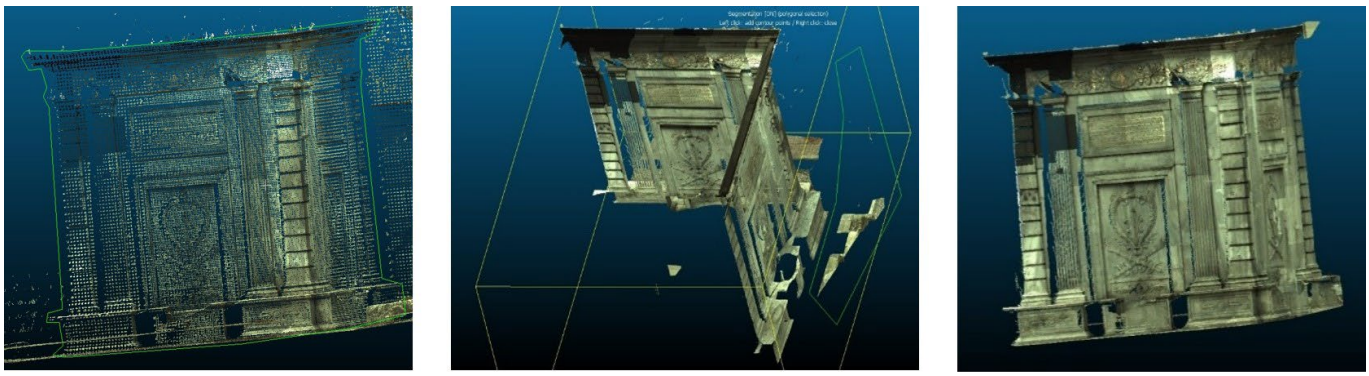

(a) (b) (c)

Figure 12. (a) selection of points belonging to the structure, (b) detection of noise points, (c) point cloud formed by filtering noise points

7.2. Merging The Point Cloud

The registration process is performed in order to Decouple the data obtained in all scans and to ensure that all the details of the structure are contained in a single point cloud. In order for the 3D model to be created precisely, the common surfaces are combined with the matching of control points. Since each successive front screening is carried out by having common control points with each other, matching common control points allows a more accurate model to be created.

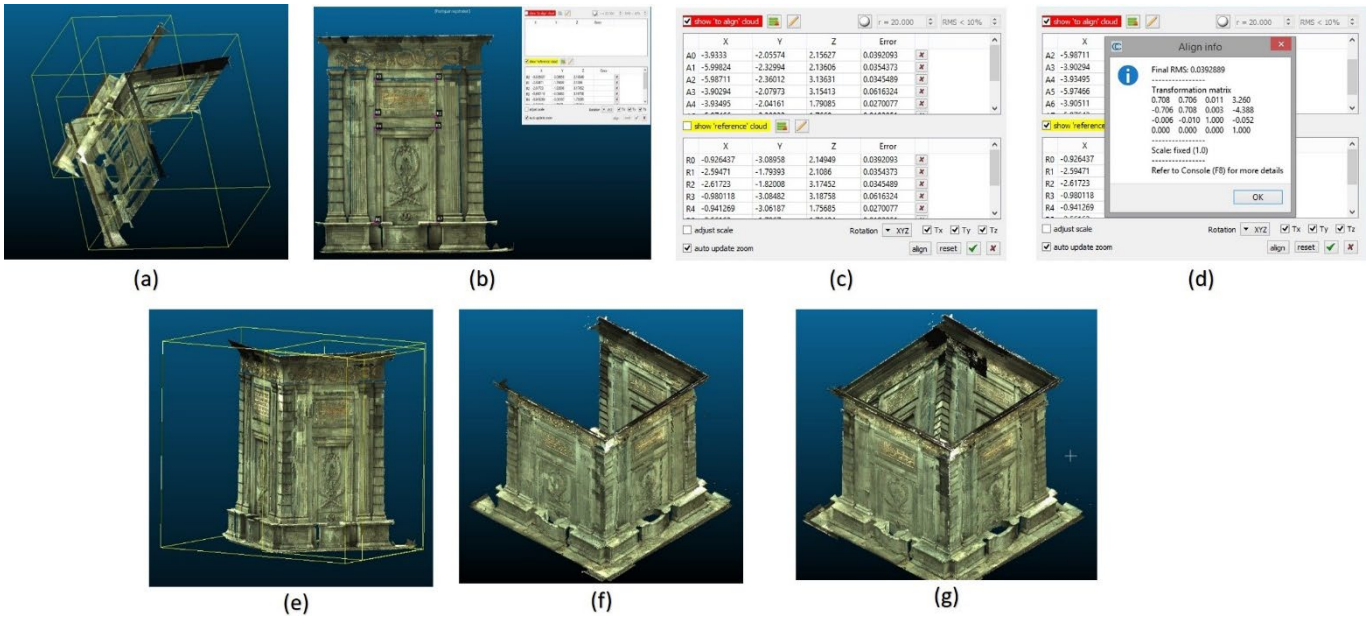

Figure 13. (a) displaying the scan data to be mapped in local coordinates, (b) selecting the control points located on the structure, (c) display of coordinate values in a local coordinate system as a result of selecting control points determined on surfaces with a common scanning area, (d) the align info values obtained at the end of the merge operation are (Final RMS, Transformation matrix and Scale fixed), (e) two facades mapped using checkpoints, (f) three facades mapped using checkpoints, (g) mapping and creating all facades of the structure in a 3D model

8. Results

With the 3D point cloud created, Bezmialem Valide Sultan Fountain will be able to be used as base data in the restoration work that will be carried out to restore it to its former state if it is damaged in any case. When we look at the advantageous side of the process performed, it is ensured that data can be obtained faster and with more precise accuracy compared to classical methods. The roof of the structure was not included in the model because it was not scanned. In order for the roof part to be included in the model, the scanning process can be performed with the help of a drone, and the obtained scanning data can be integrated into the model in the point cloud belonging to the roof. It can be determined how sensitive a model has been created by performing an accuracy analysis of the operations performed. The accuracy of the created model can be determined in future studies.

9. Discussion

By using the CloudCompare software, the point cloud of the desired structure is obtained as a result of clearing the noise points contained in the point clouds obtained as a result of different sessions. After cleaning the noise points, a 3D model of the structure is formed by combining the point clouds obtained, but it is necessary to scan the roof parts with the help of a drone, and thus the model of the structure can be fully realized.

10. Conclusion

By making a comparison with a reference 3D model, the accuracy analysis of the 3D model obtained as a result of the study will be performed and the accuracy of the result data will be determined.

Acknowledgement

This study was partly presented at the 7th Advanced Engineering Days.

Author contributions

Conceptualization and design: Berkan Sarıtaş
Data collection: Umut Aydar; Analysis of data and interpretation of results: Berkan Sarıtaş, Beyza Karademir; Writing the first draft of the manuscript: Berkan Sarıtaş, Umut Aydar; Review and editing: Berkan Sarıtaş, Umut Aydar

Conflicts of interest

There is no conflict of interest between the authors.

Statement of Research and Publication Ethics

Research and publication ethics were complied with in the study.

References

Alptekin, A., & Yakar, M. (2020). Kaya bloklarının 3B nokta bulutunun yersel lazer tarayıcı kullanarak elde edilmesi. *Türkiye LİDAR Dergisi*, 2(1), 1-4.

Alptekin, A., Fidan, Ş., Karabacak, A., Çelik, M. Ö. & Yakar, M. (2019). Üçayak Örenyeri'nin yersel lazer tarayıcı kullanılarak modellenmesi. *Turkey Lidar Journal*, 1(1), 16-20.

Altuntaş C. & Yıldız F. (2008). Yersel Lazer Tarayıcı Ölçme Prensipleri ve Nokta Bulutlarının Birleştirilmesi. *Jeodezi ve Jeoinformasyon Dergisi*. 98, 20-27.

Balcı, D. (2022). Kültürel Mirasın Belgelenmesinde Lazer Tarayıcıların Kullanılması. *Türkiye Lidar Dergisi*, 4(1), 27-36

Boehler, W. & Marbs, A. (2002). 3D Scanning Instruments. In Proceedings of International Workshop on Scanning for Cultural Heritage Recording – Complementing or Replacing Photogrammetry. Corfu, Greece, September, 1 – 2.

Erdoğan, A., Kabadayı, A. & Akın, E. S. (2021). Kültürel Mirasın Fotogrametrik Yöntemle 3B Modellenmesi: Karabıyık Köprüsü Örneği. *Türkiye İnsansız Hava Araçları Dergisi*, 3(1), 23-27. DOI: 10.51534/tiha.911147

Fidan, Ş. & Ulvi, A. (2022). Tarsus Aziz Pavlus Kilisesinin Yersel Lazer Tarama Teknikleri ile Üç Boyutlu Modelinin Oluşturularak Sanal Gerçekliğe Hazırlamanın Değerlendirilmesi. *Türkiye Lidar Dergisi*, 4(2), 60-70

Forkuo E. K. & King B. (2004). Automatic Fusion of Phtogrammetric Imagery And Laser Scanner Point Cloud, ISPRS XXth Congress, Commission 4, s.921-926, Istanbul, 12-23 July.

Gümüş, K. & Erkaya, H. (2007). Mühendislik Uygulamalarında Kullanılan Yersel Lazer Tarayıcı Sistemler. 11. Türkiye Harita Bilimsel ve Teknik Kurultayı, 2-6 Nisan, Ankara

Kanun, E., Metin, A. & Yakar, M. (2021). Yersel Lazer Tarama Tekniği Kullanarak Ağzıkara Han'ın 3 Boyutlu Nokta Bulutunun Elde Edilmesi. *Türkiye Lidar Dergisi*, 3(2), 58-64. DOI: 10.51946/melid.1025856

Kaya, Y., Şenol, H. İ. & Polat, N. (2021b). Threedimensional modeling and drawings of stone column motifs in Harran Ruins. *Mersin Photogrammetry Journal*, 3(2), 48-52.

Kaya, Y., Polat, N., Şenol, H. İ., Memduhoglu, A. & Ulukavak, M. (2021). Arkeolojik kalıntıların belgelenmesinde yersel ve İHA fotogrametrisinin birlikte kullanımı. *Türkiye Fotogrametri Dergisi*, 3(1), 09-14

Kabadayı, A. (2023). Yersel lazer tarama yöntemi ile röleve ve restütasyon projelerinin hazırlanması; Akşehir kale kalıntısı örneği. *Türkiye LİDAR Dergisi*, 5(1),17-25.

Korumaz, A. G., Dülgerler, O. N. & Yakar, M. (2011). Kültürel Mirasin Belgelenmesinde Dijital Yaklaşımlar. *Selçuk Üniversitesi Mühendislik, Bilim ve Teknoloji Dergisi*, 26(3), 67-83.

Liu, X. (2008). Airborne LiDAR for DTM generation: Some critical issues. *Progress in Physical Geography*, 32(1), 31-49.

Lichti, D. D. & Gordon, S. J. (2004). Error Propagation in Directly Georeferenced Terrestrial Laser Scanner Poin Clouds for Cultural Heritage Recording, Proceedings of FIG Working Week, s.on CD, Athens, Greece, 22-27 May.

Meng, X., Currit, N. & Zhao, K. (2010). Ground filtering algorithms for airborne LiDAR data: A review of critical issues. *Remote Sensing*, (2), 833-860.

Memduhoglu, A., Şenol, H. İ., Akdağ, S. & Ulukavak, M. (2020). 3D Map Experience for Youth with Virtual/Augmented Reality Applications. *Harran Üniversitesi Mühendislik Dergisi*, 5(3), 175-182.

Mettenleiter, M., Härtl, F., Frölich, C. & Langer, D. (2000). Imaging Laser Radar for 3DModelling of Real World Environments. Internat. Conference on OPTO/IRS2/MTT. Erfurt, Germany, May 9 – 11

Mills, J. & Barber, D. (2003). An Addendum to the Metric Survey Specifications for English Heritage – the collection and archiving of point cloud data obtained by terrestrial laser scanning or other methods. Version 11/12/2003.

Polat, N., Önal, M., Ernst, F. B., Şenol, H. İ., Memduhoglu, A., Mutlu, S., ... & Kara, H. (2020). Harran Ören Yeri Arkeolojik Kazı Alanınından Çıkarılan Bazı Küçük Arkeolojik Buluntuların Fotogrametrik Olarak 3B Modellenmesi. *Türkiye Fotogrametri Dergisi*, 2(2), 55-59.

Polat, N. & Uysal, M. (2016). Hava Lazer Tarama Sistemi, Uygulama Alanları ve Kullanılan Yazılımlara Genel Bir Bakış

Sarı, B., Hamal, S. N. G. & Ulvi, A. (2020). Documentation of complex structure using Unmanned Aerial Vehicle (UAV) photogrammetry method and Terrestrial Laser Scanner (TLS). *Turkey Lidar Journal*, 2(2), 48-54.

Staiger, R. (2003). Terrestrial Laser Scanning Technology, Systems and Applications, FIG Regional Conference. Marrakech, Morocco, December 2-5, 2003.

Şenol, H. İ., Polat, N., Kaya, Y., Memduhoğlu, A. & Ulukavak, M. (2021). Digital documentation of ancient stone carving in Şuayip City. *Mersin Photogrammetry Journal*, 3(1), 10-14.

Ulvi, A. & Yiğit, A. Y. (2019). Kültürel Mirasın Dijital Dokümantasyonu: Taşkent Sultan Çeşmesinin Fotogrametrik Teknikler Kullanarak 3B Modelinin Yapılması. *Türkiye Fotogrametri Dergisi*, 1(1), 1-6.

Ulvi, A., Yakar, M., Yiğit, A. Y. & Kaya, Y. (2020). İHA ve yersel fotogrametrik teknikler kullanarak Aksaray Kızıl Kilise'nin 3 Boyutlu nokta bulutu ve modelinin üretilmesi. *Geomatik Dergisi*, 5(1), 22-30.

Us, H., Köse, S. & Bıyık, M. E. (2022). Antik Mezar Taşlarının Yersel Lazer Tarama (YLT) Yöntemi ile Üç Boyutlu (3B) Belgelenmesi. *Türkiye Lidar Dergisi*, 4(1), 11-16

Yakar, M., Yıldız, F. & Yılmaz, H. M. (2005). Tarihi ve Kültürel Miraslarin Belgelenmesinde Jeodezi Fotogrametri Mühendislerinin Rolü. *TMMOB Harita ve Kadastro Mühendisleri Odası*, 10.

URL-1: turanakinci.com (2023). "Beşiktaş Valideçeşme Bezmialem Çeşmesi". (Date of Access: 17.06.2023). https://www.turanakinci.com/portfolio-view/besiktas-valideçesme-bezmialem-cesmesi/

URL-2: sarrafoglu.com (2016). "Bezm-i Alem Valide Sultan Çeşmesi ve Şaşırtan Hikayesi". (Date of Access:17.06.2023). https://www.sarrafoglu.com/bezm-i-alem-valide-sultan-cesmesi-ve-sasirtan-hikayesi/

Advanced LiDAR

http://publish.mersin.edu.tr/index.php/lidar/index

e-ISSN 2791-8572

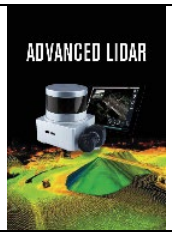

Analysis of Gümüşhane-Trabzon Highway Slope Static and Dynamic Behavior Using Point Cloud Data

Şener Ali Yazıcıoğlu[1], Kaşif Furkan Öztürk[2], Mehmet Akif Günen*[3]

[1]Gümüşhane University, Department of Mining Engineering, 29000, Gümüşhane, Türkiye; (s.aliyazicioglu@gumushane.edu.tr)
[2]Gümüşhane University, Department of Civil Engineering, 29000, Gümüşhane, Türkiye; (kasiffurkan.ozturk@gumushane.edu.tr)
[3]Gümüşhane University, Department of Geomatics Engineering, 29000, Gümüşhane, Türkiye; (akif@gumushane.edu.tr)

Keywords

Photogrammetry,
Slope stability,
Point cloud,
Dynamic analysis.

Research Article

Received : 15.09.2023
Revised : 20.09.2023
Accepted : 26.09.2023
Published : 30.09.2023

* **Corresponding Author**
akif@erciyes.edu.tr

Abstract

It is common knowledge that snowmelt, excessive precipitation, naturally occurring or man-made faulty applications, and static loading conditions can weaken slope stability, which can result in numerous fatalities and property damage. Then again, it is referred to that a few disastrous earthquakes, for example, 1999 Izmit (Mw=7.1), 2023 Pazarcık (Mw=7.7) and Elbistan (Mw=7.6) that happened because of the way that our country is situated in the earthquake belt trigger the slope stability. Within this scope, the mass moves that might happen on the slopes because of the earthquake might cause loss of life and property as well as prevention of road transport. In light of the earthquake, it is critical to guarantee that intercity highways will continue to be serviceable. In this paper, a 3D point cloud was made utilizing photogrammetrically high-resolution aerial photographs and a primer examination of a selected slope system was performed in the Zigana region of the Gümüşhane-Trabzon highway (the previous Zigana Tunnel 5 km). The noise of the point cloud made by utilizing morphological and statistical sorting filters is excluded. Within the relevant point cloud, a section was created from the 3D surface of a region. By using this section, slope stability analysis were implemented for static and dynamic loading situations of the slope by taking into account some foundation rock parameters that are thought to represent the region. In this study, the effect of earthquake induced dynamic analyses on stability were investigated comparatively. As a result of the selected parameters, it is observed that the road slopes that appear to be stable can become unstable especially with the earthquake effect.

1. Introduction

The stability of slopes may deteriorate due to various reasons in nature. Some of these may occur due to natural causes such as strong earthquakes, weathering of rocks or soils, increase in pore water pressure caused by excessive rainfall or water saturation of soils that are not saturated with water, while some of them may occur due to unconscious engineering activities.

It may cause failure of slope stability systems that are already significantly stable or moderately stable under seismic loading (Kramer, 1996). Earthquakes may create greater damage to building systems than their current effects due to loss of slope stabilities (Youd, 1987; Wilson and Keefer, 1985). It has been observed that the loss of life in the major earthquakes that took place in Japan between 1964 and 1980 was largely due to landslides triggered by earthquakes (Kobayashi, 1981). The Haiyuan earthquake in China triggered hundreds of landslides and caused more than 100,000 deaths. During the 1999 Düzce earthquake, a landslide that took place in the Bakacak region, approximately 15 km west of Bolu province, caused an almost 100 m long section slide of the highway and spread over the valley (Bakir and Akiş, 2001). For this reason, transportation was disrupted for a few days until an alternative route was opened (Erdik, 2001). Technical reports prepared on the Pazarcık (Mw=7.7) and Elbistan (Mw=7.6) earthquakes that occurred in 2023 revealed slope stability problems ranging from a few meters to hundreds of meters in length (Çetin et al., 2023).

Cite this;

Yazıcıoğlu, A. Ş., Öztürk, F. K. & Günen, M. A. (2023). Analysis of Gümüşhane-Trabzon Highway Slope Static and Dynamic Behavior Using Point Cloud Data. Advanced LiDAR, 3(2), 70-75.

Slope stability systems can generally be considered in two ways. First of these is to analyze the slope stability in case of static loading. In such a case, the balance of system is generally associated with external loading/unloading operations in ground system's own weight. In the second of these, in addition to static loading, the slope stability system is investigated by assuming that slopes are exposed to dynamic loading. In this case, it is possible to define the frequently preferred methods under two headings: a) limit equilibrium method and b) numerical methods based on finite elements or finite differences.

For both methods, factor of safety for slopes can be determined. In both approaches, the situation regarding slope safety can be determined by calculating the factor of safety. In many studies conducted in this context, it is often observed that while stability analyzes of ground systems are carried out, whether the slope is generally safe or not is examined by calculating the factor of safety for slopes (Dawson et al., 1999; Matsui and San, 1992).

The analyzes carried out within the scope of the study consist of two parts: static and pseudo-static analyses. In parametric analyses, two different rock properties were taken into account for the slope system. These expressed rock parameters were chosen based on the assumption that the slope system consists of limestone or andesitic basaltic tuff, which is known to be common in the region. Comparisons were implemented using total displacements and system's factor of safety for three node points determined from slope section produced using the data obtained from the point cloud.

2. Method

In this study, parametric analyzes were carried out with the slope section obtained using photogrammetrically produced point cloud data in the Old Zigana Tunnel region (Gümüşhane side). To produce photogrammetric data of the study area, 11 aerial images taken by the General Directorate of Mapping with an UltraCam Eagle M3 camera in 2018 were used. Each image is 13080x20010 pixels in size and the camera calibration parameters presented with the images were used in the point cloud production stage. In order to carry out the geo-referencing process of the data, geographical data collection was carried out at each point, a minimum of 10 epochs, with the GeoMax Zenith15 GNSS receiver on the sharp edges of the concrete structures that have not been deteriorated or changed since 2018 in the study area. The created point cloud has a ground sampling interval of 12 cm. Error values of 4 control points not used in the photogrammetric balancing process are presented in Table 1. The solid and digital terrain model representing the study area is given in Figure 1.

Table 1. Total error values of control points

	X	Y	Z
Total Error (m)	0.04	0.07	0.2

After the points representing the digital land surface covering the study area were obtained, the noisy data in the point cloud was filtered and cleaned and then transferred to the CAD environment to perform the cross-section creation process. The raw point cloud must be filtered to perform more meaningful data analysis and processing. Additionally, the point cloud must be filtered to preserve existing details such as edge features and achieve the smooth surfaces needed to produce realistic digital models of physical objects (Günen and Beşdok, 2021). For noise removal, the statistical outlier method developed by Rusu and his colleagues (Rusu et al., 2007), which assumes that the distance between a certain point and its neighbors is normally distributed, was first used. For each pi point (i=1…n) in the data set, the average ri distance is calculated by taking into account the K-nearest neighbors (K-nn). This value is evaluated using the sigma rule on the entire dataset, meaning if the result is not within N standard deviations from the mean, then the point is treated as an variance. Assuming that the average distance to K-nn is normally distributed, the standard deviation multiplier can be selected according to the cumulative distribution function from the normal distribution.

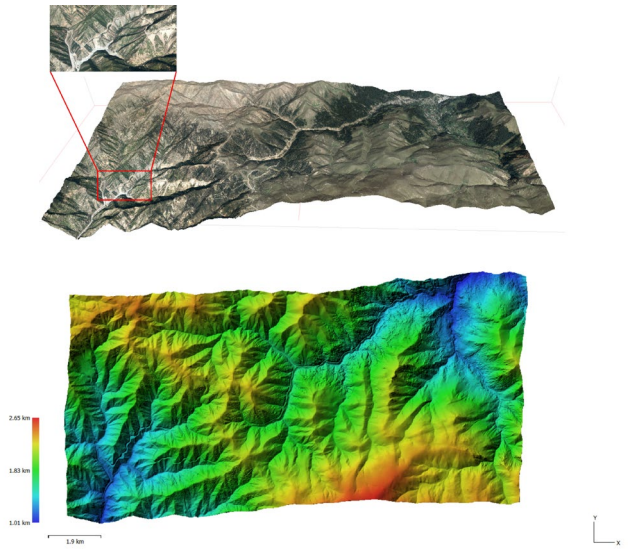

Figure 1. 3D models of the working area

Then, a morphological filter was applied to the point cloud. Morphological filtering methods often rely on extensions of digital image operators adapted to process point elevation rather than grayscale intensity. Morphological filters analyze the shapes and structures of objects in the point cloud. These filters are often used in opening and closing steps to remove small details and noise present in the point cloud. Opening is used to remove small objects or details. Closing is used to preserve the shapes and boundaries of large objects. These steps help to obtain a clearer and cleaner point cloud by determining the shapes of objects in the point cloud more accurately. In the progressive morphology filtering method used in this study, the filtering process depends on the window size and height difference threshold. As a result of an iterative process, points of outer place objects of different sizes are removed from the data set while preserving the ground data (Tan et al., 2018, Wang et al., 2014). Figure 2 shows the trimmed point cloud of the study area and the solid model

representation of the point cloud that was spatially sampled again after filtering.

The rock data used in parametric analyzes were considered as limestone and andesitic basaltic tuff, which are known to be common in the region (Korkmaz, 1988). The physical and mechanical properties used for rock parameters are given in the Table 2. Additionally, poisson ratio were considered as 0.23 and 0.26 for limestone and andesitic basaltic tuff, respectively (Briaud, 2013; Alkan and Dağ, 2018).

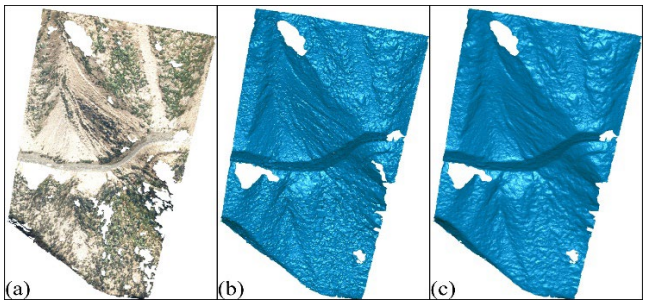

Figure 2. a) Colored b) 2m resolution c) filtered solid model of the working area

Table 2. Rock parameters used in analysis (Korkmaz, 1988)

Rock Type	E_{dyn}, MPa	c, MPa	ϕ (°)	γ, kN/m^3
Limestone	61978	25.497	50	27.26
Andesitic basaltic tuff	28341	17.161	46	25.95

E_{dyn}: Dynamic modulus of elasticity, c: Cohesion, ϕ: Angle of internal friction, γ: Unit volüme weight

2.1. Finite Element Analysis

The finite element method (Bentley, 2020) was used in the stability analysis of the slope system. Two stages were followed in the analyses performed. In the first stage (initial stage), the behavior of the slope system under its own weight was performed by gravity weight. By preserving the effective stresses produced using this approach, in the second stage, the unusual deformations occurring in the slope system are reset and safety analysis is performed to calculate the factor of safety coefficient. Starting from the initial stage, in addition to pseudo-static analyses, analyses were carried out for the factor of safety gradually. In pseudo-static analyses, pseudo-acceleration coefficients are multiplied by g=9.81 m/s^2 and applied to the center of gravity of the area with sliding potential. With this approach, the slope system that will be exposed to earthquake is loaded by "g". It can be considered that horizontal acceleration coefficient (kh) for "large" earthquakes is 0.1, for "severe, destructive" earthquakes is 0.2 and for disaster level is 0.5. In this context within the scope of the study, pseudo-static analyzes were carried out, regarding as 0.1g increments from 0.1g to 0.5g.

Nonlinear behavior of the rocks was considered with the Mohr-Cloumb elasto-plastic material model in the analyses. In the expressed material model, in addition to mechanical properties such as modulus of elasticity and Poisson's ratio, which are frequently used for the linear behavior of the material; cohesion, internal friction angle and dilation angle must be included. Within the scope of the study, dilation angle was accepted as zero. The side boundaries and base of the model were enlarged to eliminate convergence problems, and base was assumed to be the bedrock. While horizontal movement is not allowed at the nodes on the sides, the movement of the nodes on the base is kept in all directions. The network distribution used in the analysis and the nodes where the responses are obtained in the model are presented in Figure 3 and Figure 4, respectively.

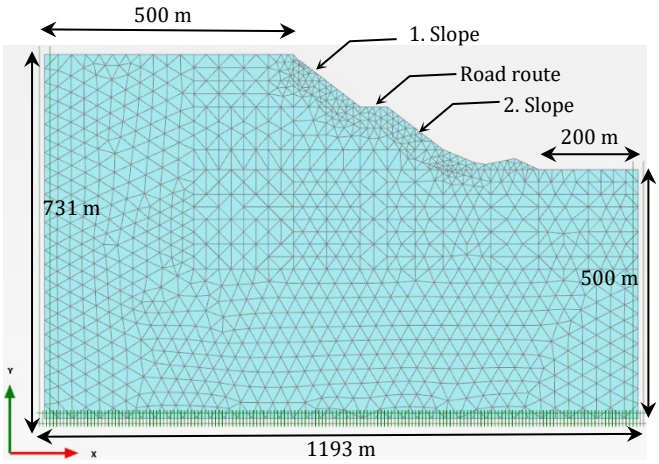

Figure 3. Network distribution for slope model

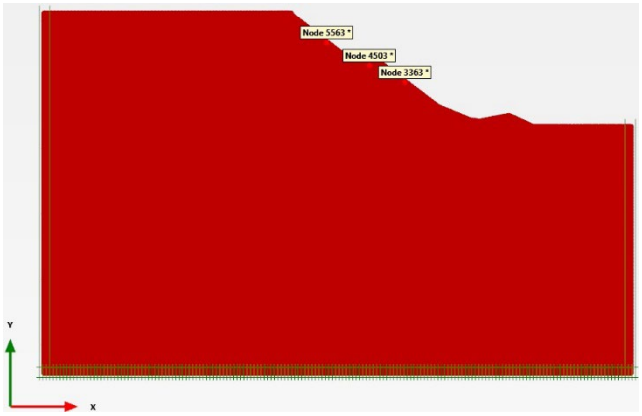

Figure 4. Selected nodes

3. Results and Discussion

3.1. Displacements Obtained from Pseudo-Static Analyzes

The relationship between the largest displacements and loadings obtained from selected nodes in the slope system using limestone and andesitic basaltic tuff system is presented in Figure 5 and Figure 6, respectively. It is clearly understood that the changes generally show an increasing trend in both ways depending on the increase in loadings.

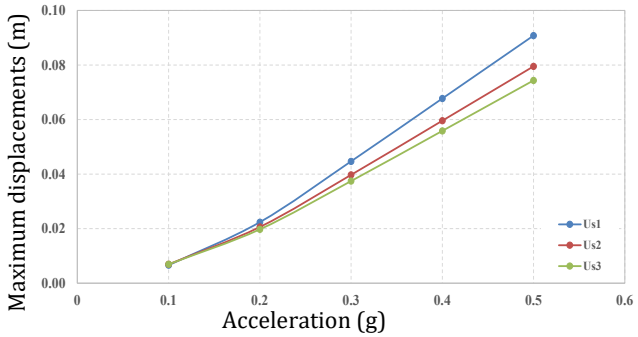

Figure 5. The relationship between the largest displacements and loadings obtained from the selected nodes for limestone

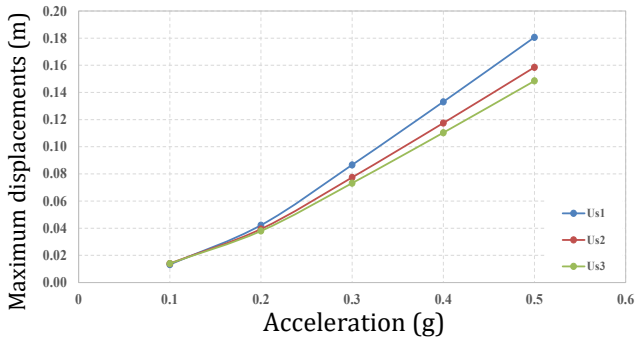

Figure 6. The relationship between the largest displacements and loadings obtained from selected nodes for andesitic basaltic tuff

Table 3. Displacements derived from limestone

Acceleration	Us1(m)	Us2(m)	Us3 (m)
0.1g	0.007	0.007	0.007
0.2g	0.022	0.021	0.020
0.3g	0.045	0.040	0.037
0.4g	0.068	0.060	0.056
0.5g	0.091	0.080	0.074

g=9.81 m/s^2,
Us1:the largest displacement obtained from the node no. 5563,
Us2:the greatest displacement obtained from the node no. 4503,
Us3=the greatest displacement obtained from the node no. 3363

Table 4. Displacements obtained from andesitic basaltic tuff

Acceleration	Us1(m)	Us2(m)	Us3 (m)
0.1g	0.013	0.014	0.014
0.2g	0.042	0.039	0.038
0.3g	0.087	0.077	0.073
0.4g	0.133	0.117	0.110
0.5g	0.181	0.159	0.149

It is observed that under the applied loading, the displacements in the slope system for limestone and andesitic basaltic tuff increase significantly, showing a general trend (Figure 5 and Figure 6). For example, while the Us1 displacement obtained from the 1st slope system using limestone was around 0.007 m under 0.1g loading, it is seen that the same response was obtained as 0.045 and 0.091 m, with an increase of 543% and 1200% under 0.3g and 0.5g loading, respectively (Table 3). Another example of this situation can be given using the Us2 or Us3 displacements in Table 3. For example, while the Us3 displacement obtained from the 2nd slope system was 0.007 m under 0.1g loading, the same response was obtained as 0.037 m and 0.074 m with an increase of 429% and 957% under 0.3g and 0.5g loading, respectively.

The largest displacements obtained from pseudo-static analyzes carried out in the slope system, considering andesitic basaltic tuff, are presented in Table 4. As can be clearly understood here, the increase in loading generally significantly increases the largest displacements obtained from selected nodes. For example, while the Us1 displacement obtained from the 1st slope system is 0.013 m under 0.1g loading, the same displacement becomes 0.087 m and 0.181 m with an increase of 569% and 1292% under 0.3g and 0.5g loading, respectively. It is possible to obtain a similar increasing trend within the selected node on the route. For example, while the Us2 displacement is 0.014 m under 0.1g loading, the same displacement value is obtained as 0.077 m and 0.159 m under 0.3g and 0.5g loadings, increasing by 450% and 1036%, respectively.

Another point that should be emphasized here is that the displacements obtained from the selected nodes, considering limestone and andesitic basaltic tuff, vary significantly compared to each other. For example, while the Us1 displacement was obtained as 0.007 m under 0.1g loading for limestone, this displacement for the same loading was achieved around 0.013 m for andesitic basaltic tuff, with an increase of 86% due to the decrease in the mechanical properties of the rock system and the unit volume weight. This change shows a similar trend, increasing by 93% and 99% under 0.3g and 0.5g loadings, respectively. (Table 3 and Table 4).

3.2. Factor of Safety Coefficient Obtained Under Loadings

The changes in the security numbers obtained from the analyzes are shown in Figure 7 and Figure 8. When Figure 7 and Figure 8 are examined, it is understood that the safety numbers obtained from limestone and andesitic basaltic tuff show a continuous downward trend from the static loading condition in the slope system to the 0.5g loading condition. In order to obtain a constant value of safety numbers in the slope system, it is seen that 100 steps for limestone and 1000 steps for andesitic basaltic tuff are sufficient under loading conditions.

The factor of safety obtained from the analyzes carried out using limestone and andesitic basaltic tuff for the slope system are shown in Table 5. When Table 5 is analyzed, it is clearly seen that the decreasing trend of safety numbers from static loading to pseudo-static loading. For example, while the factor of safety for slope system created from limestone is around 29.33 in static condition, it is seen that the same factor of safety is obtained at 21.62, 13.45 and 9.51 with a decrease of 26%, 54% and 67.5% under 0.1g, 0.3g and 0.5g loadings, respectively. It is possible to see a similar decreasing trend in the slope system created from the andesitic basaltic tuff system. For example, while the static factor of safety for andesitic basaltic tuff is 21.60, this value is

obtained around 16.14, 9.99 and 7.10 with a decrease of 25%, 54% and 67% under 0.1g, 0.3g and 0.5g loadings, respectively.

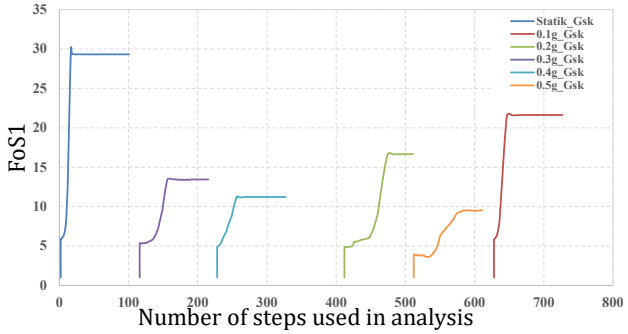

Figure 7. Relationships between step numbers and factor of safety used in the analyzes carried out considering limestone

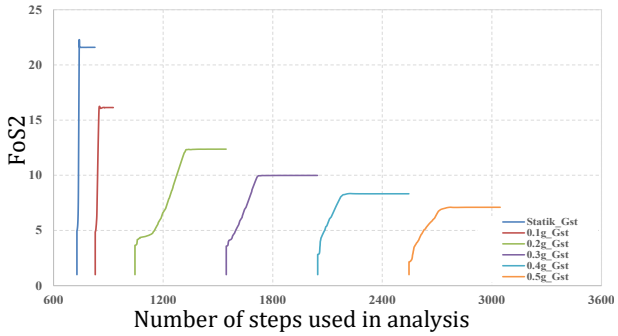

Figure 8. Relationships between step numbers and factor of safety used in the analyzes carried out considering andezitic basaltic tuff

Table 5. Factor of safety obtained from limestone and andesite-basaltic tuff

Acceleration	Gsk	Gst
Statik	29.33	21.60
0.1g	21.62	16.14
0.2g	16.66	12.37
0.3g	13.45	9.99
0.4g	11.22	8.32
0.5g	9.51	7.10

FoS1: Factor of safety for the section obtained from the analyzes performed under the loading considered for limestone
FoS2: Factor of safety for the section obtained from the analysis carried out under the loading considered for andesitic basaltic tuff rock

When a comparison is made between the FoS values obtained for limestone and andesitic basaltic tuff, it is clearly seen that the FoS values obtained from limestone are greater than the FoS values obtained for andesitic basaltic tuff for all loading conditions (Table 5). For example, while the FoS values obtained from andesitic basaltic tuff for the static situation is 21.60, it is seen that the same FoS value is 29.33. In this example, it can be seen that the FoS value obtained from limestone has increased by around 36% compared to the FoS value obtained from andesitic basaltic tuff. Similar changes can be easily observed in pseudo-static loading. For example, if we look at the FoS values obtained for 0.1g, 0.3g and 0.5g for andesitic basaltic tuff, these values are obtained at 16.14, 9.99 and 7.10, while the same values for limestone are 16.14, 35% and 34% with increases of around 33%, 35% and 34%. It is seen that 9.99 and 7.10 were obtained.

Considering that unstable situation for the stability status of the slopes will occur below 1 and it is understood that under the analyzed assumptions, the slope system is stable under both static and pseudo-static loading if it consists of limestone or andesitic basaltic tuff system.

4. Conclusion

Within the scope of this study, a slope section was obtained using photogrammetrically produced point cloud data in the Zigana region of the Gümüşhane-Trabzon highway (5 km Gümüşhane side of the old Zigana Tunnel). Parametric analyzes were carried out for the created slope system to be limestone or andesitic basaltic tuff, which is known to be frequently found in the region. Finite element approach was considered for parametric analyses. Loadings were carried out under static and Pseudo-static loadings. In pseudo-static analyses, the load condition was increased from 0.1g to 0.5g. The data obtained from the analyzes are presented in terms of total displacements obtained from three selected nodes. Additionally, factor of safety values was calculated for static and pseudo-static loading cases. The inferences obtained in this context are listed below.

For cases where the slope system consists of limestone or andesitic basaltic tuff, the displacements obtained from pseudo-static loading can increase significantly within the three nodal points depending on the increase in the loading magnitude.

Displacements can increase significantly due to the decrease in mechanical parameters and unit volume weight of andesitic basaltic tuff compared to limestone for all pseudo-static loading conditions.

When the factor of safety values calculated under the assumptions made are examined, it is understood that the slope system is stable (durable) under both static and pseudo-static loading in cases of limestone or andesitic and basaltic tuff. The change in factor of safety decreases significantly in both cases due to the gradual increase in loadings. It is also noteworthy that factor of safety of the slope created from andesitic basaltic tuff remains relatively lower for all loading conditions compared to limestone.

Author contributions

ŞA was involved in writing, investigation and analysis, KFÖ was involved in conceptualization, validation and writing, MAG was involved in ideating, language checking and editing

Conflicts of interest

The authors declare no conflicts of interest.

Statement of Research and Publication Ethics

Research and publication ethics were complied with in the study.

Acknowledgments

Abstract of this study TUFUAB XII. Presented at the Technical Symposium.

References

Alkan, F. & Dağ, S. (2018). Gümüşhane yöresinde yüzeylenen magmatik kökenli bazı kayaların jeomekanik özellikleri arasındaki ilişkilerin araştırılması. *Uludağ Üniversitesi Mühendislik Fakültesi Dergisi*, *23*(2), 203-216.

Bakır, B. S. & Akış, E. (2005). Analysis of a highway embankment failure associated with the 1999 Düzce, Turkey earthquake. *Soil Dynamics and Earthquake Engineering*, 25(3), 251-260.

Bentley, PLAXIS 2D-Tutorial Manual, 2020

Briaud, J. L. (2013). Geotechnical engineering: unsaturated and saturated soils. John Wiley & Sons.

Çetin, K. Ö., Gökçeoğlu, C., Moss, R. E. S., Ilgaç, M.,Can, G., Çakır, E., Aydın, B. U., Şahin, A., Türkezer, M., Söylemez, B., Ocak, S. & Güzel, H. (2023). Geotechnical Findings and the Performance of Geo-Structures. Kemal Önder Çetin, Makbule Ilgaç, Gizem Can and Elife Çakır (Der.), Preliminary Reconnaissance Report on February 6, 2023, Pazarcık Mw=7.7 and Elbistan Mw=7.6, Kahramanmaraş-Türkiye Earthquakes içinde, Middle East Technical University.

Dawson, E. M., Roth, W. H. & Drescher, A. (1999). Slope stability analysis by strength reduction. Geotechnique, 49(6), 835-840.

Erdik, M. (2001). Report on 1999 Kocaeli and Düzce (Turkey) earthquakes. *In Structural control for civil and infrastructure engineering*, 149-186.

Günen, M. A. & Beşdok, E. (2021). Comparison of point cloud filtering methods with data acquired by photogrammetric method and RGB-D sensors. International Journal of Engineering and Geosciences, 6(3), 125-135.

Kobayashi, Y. (1981). Causes of fatalities in recent earthquakes in Japan. *Natural disaster science*, 3(2), 15-22.

Korkmaz, T. (1988). Maçka-Gürgenağaç (Trabzon) yeni yol şevlerinin duraylılık açısından incelenmesi (Yüksek lisans tezi, Fen Bilimleri Enstitüsü).

Kramer, S. L. (1996). Geotechnical earthquake engineering. Pearson Education India.

Matsui, T. & San, K. C. (1992). Finite element slope stability analysis by shear strength reduction technique. *Soils and foundations*, 32(1), 59-70.

Rusu, R. B., Blodow, N., Marton, Z., Soos, A. & Beetz, M., (2007). Towards 3D object maps for autonomous household robots. IEEE/RSJ international conference on intelligent robots and systems.

Tan, Y., Wang, S., Xu, B. & Zhang, J. (2018). An improved progressive morphological filter for UAV-based photogrammetric point clouds in river bank monitoring. *ISPRS Journal of Photogrammetry and Remote Sensing*, 146, 421-429.

Terzaghi, K. (1950). Mechanism of landslides, Enginnering Geology (Berkeley) Volume.

Youd, T. L. (1978). Major Cause of a Earthquake Damage Is Ground Failure. *Civil Engineering*, 48(4).

Wang, Q., Wu, L., Xu, Z., Tang, H., Wang, R. & Li, F. (2014). A progressive morphological filter for point cloud extracted from UAV images. IEEE Geoscience and Remote Sensing Symposium (s. 2023-2026).

Wilson, R. and Keefer, D. K. (1985). Predicting areal limit of earthquake-induced landsliding, evaluating eathquake hazards in the Los Angeles region-an earth-science perspective. *US Geological Survery Professional Paper,* 1360, 317-345.